Vertical structure of mesoscale eddies in the eastern South Pacific Ocean: A composite analysis from altimetry and Argo profiling floats

Alexis Chaigneau, Marie Le Texier, Gérard Eldin, Carmen Grados, Oscar Pizarro

Tide gauge-based sea level variations since 1950 along the Norwegian and Russian coasts of the Arctic Ocean: Contribution of the steric and mass components

O. Henry,[1] P. Prandi,[2] W. Llovel,[3] A. Cazenave,[1] S. Jevrejeva,[4] D. Stammer,[5] B. Meyssignac,[1] and N. Koldunov[5]

Received 28 October 2011; revised 11 May 2012; accepted 13 May 2012; published 27 June 2012.

[1] We investigate sea level change and variability in some areas of the Arctic region over the 1950–2009 period. Analysis of 62 long tide gauge records available during the studied period along the Norwegian and Russian coastlines shows that coastal mean sea level (corrected for Glacial Isostatic Adjustment and inverted barometer effects) in these two areas was almost stable until about 1980 but since then displayed a clear increasing trend. Until the mid-1990s, the mean coastal sea level closely follows the fluctuations of the Arctic Oscillation (AO) index, but after the mid-to-late 1990s the co-fluctuation with the AO disappears. Since 1995, the coastal mean sea level (average of the Norwegian and Russian tide gauge data) presents an increasing trend of ∼4 mm/yr. Using in situ ocean temperature and salinity data down to 700 m from three different databases, we estimated the thermosteric, halosteric and steric (sum of thermosteric and halosteric) sea level since 1970 in the North Atlantic and Nordic Seas region (incomplete data coverage prevented us from analyzing steric data along the Russian coast). We note a strong anti-correlation between the thermosteric and halosteric components both in terms of spatial trends and regionally averaged time series. The latter show a strong change as of ∼1995 that indicates simultaneous increase in temperature and salinity, a result confirmed by the Empirical Orthogonal Function decomposition over the studied region. Regionally distributed steric data are compared to altimetry-based sea level over 1993–2009. Spatial trend patterns of observed (altimetry-based) sea level over 1993–2009 are largely explained by steric patterns, but residual spatial trends suggest that other factors contribute, in particular regional ocean mass changes. Focusing again on Norwegian tide gauges, we then compare observed coastal mean sea level with the steric sea level and the ocean mass component estimated with GRACE space gravimetry data and conclude that the mass component has been increasing since 2003, possibly because of the recent acceleration in land ice melt.

Citation: Henry, O., P. Prandi, W. Llovel, A. Cazenave, S. Jevrejeva, D. Stammer, B. Meyssignac, and N. Koldunov (2012), Tide gauge-based sea level variations since 1950 along the Norwegian and Russian coasts of the Arctic Ocean: Contribution of the steric and mass components, *J. Geophys. Res.*, *117*, C06023, doi:10.1029/2011JC007706.

1. Introduction

[2] During the past few decades, the Arctic region has warmed at a faster rate than the rest of the globe in response to anthropogenic climate change [*Intergovernmental Panel on Climate Change*, 2007]. Air temperature increase [e.g., *Bekryaev et al.*, 2010; *Chylek et al.*, 2010], sea ice extent and thickness decrease [e.g., *Kwok et al.*, 2009; *Stroeve et al.*, 2007] and Greenland ice sheet mass loss [e.g., *Holland et al.*, 2008; *Steffen et al.*, 2010; *Rignot et al.*, 2011] are now among the most visible effects of global warming in the Arctic region. Other phenomena have been reported as well, such as permafrost thawing [*Lawrence et al.*, 2008], drying of Siberian lakes [*Smith et al.*, 2005], Arctic Ocean surface warming [*Karcher et al.*, 2003; *Polyakov et al.*, 2005], decline in snow cover and lake ice [*Lemke et al.*, 2007], etc.

[3] Several studies have been dedicated to study Arctic sea level along the Russian coastlines [*Proshutinsky et al.*, 2001, 2004, 2007a, 2011]. *Proshutinsky et al.* [2004] estimated sea level change using data from Russian tide gauges released in

[1]LEGOS-OMP, Centre National de la Recherche Scientifique, Toulouse, France.
[2]Collecte Localisation Satellites, Ramonville, France.
[3]Jet Propulsion Laboratory, California Institute of Technology, Pasadena, California, USA.
[4]National Oceanography Centre, Liverpool, UK.
[5]Institute of Marine Sciences, University of Hamburg, Hamburg, Germany.

Corresponding author: O. Henry, LEGOS-OMP, Centre National de la Recherche Scientifique, 14 Ave. Edouard Belin, Toulouse F-31400, France. (olivier.henry@legos.obs-mip.fr)

0148-0227/12/2011JC007706

2003 by the Arctic and Antarctic Research Institute in St Petersburg (Russia). These authors found that over the period 1950–2000, the mean sea level along the Russian coastlines rose at a mean rate of 1.85 mm/yr after correcting for the Glacial Isostatic Adjustment (GIA) process. They estimated the different contributions to this rate of rise. Using an ocean model [*Häkkinen and Mellor*, 1992], they reported a contribution of 35% for the steric effects (due to ocean temperature and salinity variations). Decrease in atmospheric sea level pressure was found to account for 30% of the observed trend while winds had a minor role, accounting for ∼10% to the trend. Since then, the state of the sea level in the Siberian sector of the Arctic Ocean is provided annually by *Proshutinsky et al.* [2007b, 2009, 2011].

[4] In the present study we revisit the sea level variations over the 1950–2009 time span, considering all available tide gauge data in the Arctic sector, north of 55°N. Thus in addition to the Russian tide gauges, we also consider tide gauge data along the Norwegian coastlines (no tide gauge records from the Canadian Arctic region are long enough to be usable). We derive mean sea level time series for these two areas and a combined "mean" sea level time series representative of the whole Eurasian sector of the coastline is produced. The present work differs from previous published studies [e.g., *Proshutinsky et al.*, 2001, 2004] in several aspects: we consider tide gauge data in a larger region (Russian and Norwegian coastlines) and estimate the steric contribution (i.e., the effects of ocean temperature and salinity variations) from observations rather than models using in situ hydrographic measurements from three different databases. Because we focus on the steric component and for the purpose of improved comparison, we correct observed sea level for GIA and atmospheric pressure loading effect. Availability of spatially distributed temperature and salinity data in the North Atlantic and Nordic Seas sectors allows us also to investigate the spatiotemporal variability in steric sea level in that region since 1970. Finally we also present spatially distributed sea level from satellite altimetry since 1993 and perform comparisons with steric data over the altimetry period, and since 2002 with GRACE (Gravity Recovery and Climate Experiment)-based ocean mass.

2. Tide Gauge Sea Level Data From the Norwegian and Russian Sectors

[5] We use monthly Revised Local Reference (RLR) tide gauge records from the Permanent Service for Mean Sea Level (PSMSL) [*Woodworth and Player*, 2003]. Data have been downloaded from http://www.psmsl.org/. These records include 11 sites along the Norwegian coast, 48 sites along the Russian coast and 3 island sites (Reykjavik, Lerwick and Torshavn). Tide gauge data from the Russian sector have been released only a few years ago (2003) and start in the 1950s. These data were used by *Proshutinsky et al.* [2004] but at that time no data beyond 1999 were available. Fortunately, updated (up to 2009) sea level data from the Russian tide gauges are now available in the PSMSL database. Information about the Russian tide gauge data and their accuracy can be found in *Proshutinsky et al.* [2007a].

[6] We consider two sets of data: (1) almost continuous records over the period 1950–2009 (hereafter data set1) and (2) combination of records covering the whole 1950–2009 period and shorter records also starting in the 1950s but ending around year 1990 (data set2). In some cases a few data gaps are observed. If the gap is less than 3 years, we linearly interpolate the missing data. Otherwise we exclude the time series. This leaves us with 27 tide gauge records for data set1 (11 sites along the Norwegian coast, 3 island sites and 13 sites along the Russian coast with almost continuous data over 1950–2009). When adding the Russian tide gauges of data set1 the shorter records all located along the Russian coastlines, we obtain data set2 corresponding to a total of 48 Russian tide gauges time series. Location and site name for the 62 sites are shown in Figure 1 and Tables 1a and 1b.

[7] There are no tide gauges along the Canadian coastlines. In the PSMSL database a few tide gauge records from this region are available but non exploitable. They were much too short and generally affected by multi decade-long gaps. We explored the possibility to collect data in other databases (i.e., Fisheries and Oceans Canada) but could not find usable data for the purpose of the present study.

[8] As we focus here on interannual to multidecadal time scales, we removed the seasonal cycles from the monthly tide gauge sea level time series, by fitting sinusoids with periods of 12 and 6 months (after closing data gaps). As this procedure may not be optimal if seasonal cycles are not purely sinusoidal, we further applied a 12-month running mean smoothing to each tide gauge time series. Figure 2 shows for two tide gauge sites (Bergen, Norway and Anderma, Russia) the raw tide gauge time series, the raw time series after removing the 12-month and 6-month sinusoids and the smoothed time series (after applying a 12-month running mean smoothing to the raw tide gauge data corrected for the 12-month and 6-month cycles).

3. Effects of Glacial Isostatic Adjustment and Atmospheric Pressure on Coastal Sea Level

[9] Because in this study we focus on the steric sea level contribution to observed sea level, the tide gauge data need to be corrected for unrelated effects such as GIA and the effect of atmospheric pressure loading. We examine below these two effects.

3.1. GIA Effect at the Tide Gauge Sites

[10] We corrected the tide gauge-based sea level for GIA. The GIA correction is crucial in the Arctic region because this effect is of the same order of magnitude as (or even larger than) the sea level rates. We used different GIA models: *Peltier*'s [2004, 2009] models with different deglaciation histories (ICE-3G and ICE-5G) and different Earth's mantle viscosity structures (VM2 and VM4). We noticed quite large differences between the models in a number of sites. To illustrate this, Figure 3 compares GIA rates in the Arctic region from the ICE-5G model for the VM2 and VM4 viscosity structures and the ICE-3G model (VM2 viscosity structure). ICE-5G model gives GIA rates of much larger amplitude than ICE-3G. To a lesser degree, some differences are also noticed between the ICE-5G VM2 and VM4 viscosity structures. To discriminate between the various solutions, we decided to choose the model version that minimizes sea level trend differences between tide gauge-based and altimetry-based data during the altimetry period (1993–2009) at the considered tide gauge sites (see section 5).

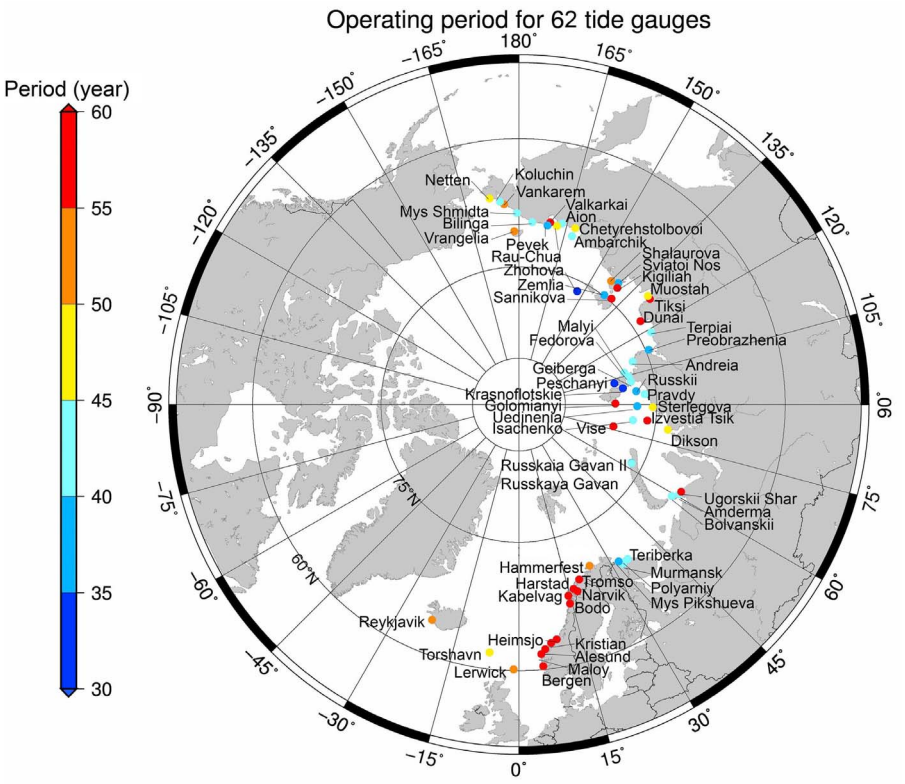

Figure 1. Distribution of the 62 tide gauges available in the Arctic region. Color indicates the length of the record in years as of 1950.

This led us to retain the ICE-5G/VM2 model to correct for GIA the tide gauge records. However, as we can see from Figure 3, differences between ICE-5G/VM2 and ICE-5G/VM4 are small in the Norwegian and Russian sectors, the region of interest in this study. In Tables 1a and 1b GIA trends (ICE5G-VM2 model) at each tide gauge site are given.

[11] Estimating the accuracy of the GIA correction is not an easy task. Some comparisons can be performed at some selected sites of the Norwegian coast between the preferred GIA correction used in this study and GPS-based crustal uplift rates. For example, using GPS precise positioning, *Vestøl* [2006] finds a crustal uplift in the range 1.2 mm/yr – 1.5 mm/yr in the southwesten part of Norway, in reasonable agreement with the ICE5G-VM2 GIA correction for the tide gauge of this area (see Tables 1a and 1b; note the reversed sign because the GIA correction is expressed in terms of equivalent sea level).

3.2. Atmospheric Pressure Loading

[12] *Proshutinsky et al.* [2001, 2004] studied in detail the effects on sea level of atmospheric loading and wind stress at the Russian tide gauge sites, using a 2-D coupled barotropic ocean-ice model (see details in the two references quoted above). Over the period 1950–1990/2000, they found that wind stress was responsible of the high frequency variability but caused insignificant trends in sea level, unlike the atmospheric pressure load that accounted for about 30% of the observed sea level trend. Unlike in *Proshutinsky et al.* [2004], we here do not correct sea level for wind stress effects. Partly this is justified since we are not interested in the high-frequency non static atmospheric response. On the other hand, changing wind-forcing results in a changing circulation which in turn leads to heat redistribution, hence to steric changes, i.e., the signal we are investigating here. Thus our preferred approach is to separately estimate steric changes, and then compare observed sea level with the steric component. On the other hand, we corrected for the static atmospheric pressure loading effect (also called inverted barometer effect, denoted IB hereafter) in the tide gauge records.

[13] To correct for the atmospheric loading effect we used surface pressure fields from the National Centers for Environmental Prediction (NCEP) [*Kalnay et al.*, 1996] (http://www.ncep.noaa. gov/), which are available on a 1.5° × 1.5° grid and at monthly intervals. To correct for the IB effect at the tide gauges sites, we tested three different methods: (1) using pressure data from the nearest grid point of the tide gauge site, (2) computing an average pressure within a 1° radius around the tide gauge, and (3) interpolating gridded pressure data at the tide gauge site. The three methods gave similar results. The IB correction was computed using the classical static correction relating sea level to surface atmospheric pressure [e.g., *Ponte*, 2006]. It should be stressed that this represents only the static response of sea level to atmospheric forcing. It is well known that dynamical effects also exist, in particular at short time scales (periods from hours to weeks) [*Wunsch and Stammer*, 1997]. Thus more realistic sea level responses to atmospheric forcing have been developed [e.g., *Carrère and Lyard*, 2003]. However, in such models, the model response is essentially similar to the static one on time scales longer than

Table 1a. Tide Gauge's Name, Country, Data Length and Location: GIA, IB and Tide Gauge Sea Level Trends at Each Tide Gauge Site (Data Set1)

Station	Country	Start–End Time	Coordinates		GIA ICE5G-VM2 (mm/yr)	IB (mm/yr)	Sea Level Trend (GIA and IB Corrected) (mm/yr)	
			Longitude (°E)	Latitude (°N)			Tide Gauge Operating Period	Altimetry Period
Reykjavik	Iceland	1956–2010	338.07	64.15	−1.23	0.21	3.42	7.43
Torshavn	Faroe Islands	1957–2006	353.23	62.02	1.31	0.37	0.11	4.76
Lerwick	United Kingdom	1950–2010	358.87	60.15	−0.12	0.24	−0.11	3.27
Maloy	Norway	1950–2010	5.12	61.93	−0.71	0.07	1.22	4.27
Bergen	Norway	1950–2010	5.30	60.40	−1.48	0.02	1.81	3.59
Alesund	Norway	1950–2010	6.15	62.47	−0.94	0.14	1.76	3.83
Kristian	Norway	1952–2010	7.73	63.12	−1.49	0.14	0.34	4.06
Heimsjo	Norway	1950–2010	9.12	63.43	−2.24	0.00	0.72	3.85
Bodo	Norway	1950–2010	14.38	67.28	−1.73	0.17	0.30	1.41
Kabelvag	Norway	1950–2010	14.48	68.22	−0.66	0.13	−0.28	2.44
Harstad	Norway	1952–2010	16.55	68.80	−1.12	0.30	−0.05	3.23
Narvik	Norway	1950–2010	17.42	68.43	−2.18	0.12	−0.29	1.67
Tromso	Norway	1952–2010	18.97	69.65	−1.30	0.27	1.09	3.16
Hammerfest	Norway	1957–2010	23.67	70.67	−1.71	0.27	2.33	4.44
Murmansk	Russia	1952–2010	33.05	68.97	−2.10	0.28	5.63	7.49
Amderma	Russia	1950–2009	61.70	69.75	−0.39	0.24	4.24	11.69
Vise	Russia	1953–2009	76.98	79.50	−2.66	0.29	2.62	0.38
Izvestia Tsik	Russia	1954–2009	82.95	75.95	−0.58	0.30	3.04	2.83
Golomianyi	Russia	1954–2009	90.62	79.55	−1.61	0.41	0.36	0.58
Dunai	Russia	1951–2009	124.50	73.93	−0.46	0.26	2.56	12.52
Tiksi	Russia	1950–2009	128.92	71.58	−0.58	0.27	2.06	6.08
Sannikova	Russia	1950–2009	138.90	74.67	−0.49	0.19	1.74	5.01
Kigiliah	Russia	1951–2009	139.87	73.33	−0.55	0.15	0.95	3.32
Aion	Russia	1954–2001	167.98	69.93	−0.36	0.08	0.96	/
Pevek	Russia	1950–2009	170.25	69.70	−0.35	0.07	3.66	8.77
Vrangelia	Russia	1950–2000	181.52	70.98	0.19	0.08	2.32	/
Vankarem	Russia	1950–2002	184.17	67.83	−0.06	0.14	2.78	/

one month. In the Arctic, the situation is more complex as non-static responses have been reported to exist on time scales between one month and one year (F. Lyard, personal communication, 2012). But for the purpose of the present study in which we focus on time scales longer than 1-year, the static response is a good approximation of the atmospheric pressure loading effect (F. Lyard, personal communication, 2012). In Figure 3 are also shown IB trends over the Arctic region (same area as for GIA) over 1950–2009. For this time span, IB trends are on the order of ∼0.5 mm/yr.

[14] In the following, we compute the IB correction at each tide gauge site using method 1. As for tide gauge-based sea level, the seasonal cycles are removed and a 12-month running mean smoothing is applied.

[15] Figure 4 shows individual tide gauge-based sea level time series in the Norwegian and Russian sectors (data set1 only) (seasonal cycles removed and further applying a 12-month running mean smoothing) corrected for GIA (ICE5G-VM2 model), with and without the IB correction. At most stations, the corrected and uncorrected curves show small differences. Accounting for the IB correction in general reduces the amplitude of the interannual variability. IB trends computed for each tide gauge operating period are presented in Tables 1a and 1b. For data set1, IB trends range between 0 and 0.3 mm/yr, except at Golomianyi (Russia) where the trend reaches 0.4 mm/yr.

[16] Tables 1a and 1b summarize tide gauge trends after correcting for GIA and IB over two time spans: the total operating period of each tide gauge and the 1993–2009 satellite operating time span.

3.3. Mean Coastal Sea Level in the Norwegian and Russian Sectors: Trend and Interannual Variability

[17] The coastal "mean" sea level (corrected for GIA and IB) (hereafter called CMSL) is displayed in Figure 5 separately for the Norwegian and Russian sectors (data sets 1 and 2) based on averages of individual time series in each region. The light gray area around each curve represents the uncertainty of the corresponding CMSL. It is computed from the root-mean squared (RMS) difference between individual time series and the mean.

[18] The Norwegian CMSL curve shows a slight downward trend between 1950 and 1975/1980, followed by an upward trend beyond 1980. The Russian CMSL curves (data sets 1 and 2) are rather similar, with an almost flat behavior between 1950 and 1975/1980 followed by an upward trend since then. This upward trend since about 1980 appears common to both Norwegian and Russian coastal regions, and thus seems to be a robust feature. For that reason, we averaged CMSL of the Norwegian and Russian sectors, plus the 3 island time series (i.e., 62 records in total) to obtain an Arctic CMSL over the whole Eurasian sector (in the following, we use the term 'Arctic CMSL' for this regional average). Arctic CMSL and associated uncertainty (computed as indicated above) over 1950–2009 is shown in Figure 6. As for the Norwegian and Russian sectors, the Arctic CMSL displays high interannual variability but almost no trend until the end of the 1970s. Subsequently it shows an increasing trend with two periods of marked rise: between 1980 and 1990 and since about 1995. The Arctic

Table 1b. Tide Gauge's Name, Country, Data Length and Location: GIA, IB and Tide Gauge Sea Level Trends at Each Tide Gauge Site (Data Set2)

			Coordinates				Sea-Level Trend (GIA and IB Corrected) (mm/yr)	
Station	Country	Start–End Time	Longitude (°E)	Latitude (°N)	GIA ICE5G-VM2 (mm/yr)	IB (mm/yr)	Tide Gauge Operating Period	Altimetry Period
Mys Pikshueva	Russia	1955–1990	32.433	69.55	−1.84	0.39	1.48	/
Murmansk II	Russia	1952–1993	33.05	68.967	−2.1	0.38	2.86	/
Murmansk	Russia	1952–2010	33.05	68.967	−2.1	0.28	5.63	7.49
Polyarniy	Russia	1950–1990	33.483	69.2	−1.46	0.23	−0.23	/
Teriberka	Russia	1950–1990	35.117	69.2	−0.7517	0.24	0.75	/
Bolvanskii	Russia	1951–1993	59.083	70.45	−0.79	0.44	3.22	/
Ugorskii Shar	Russia	1950–1989	60.75	69.817	−0.49	0.27	0.84	/
Amderma	Russia	1950–2009	61.7	69.75	−0.39	0.24	4.24	11.69
Russkaia Gavan II	Russia	1953–1993	62.583	76.183	−2.35	0.49	1.49	/
Russkaya Gavan	Russia	1953–1991	62.583	76.2	−2.37	0.31	1.28	/
Vise	Russia	1953–2009	76.983	79.5	−2.66	0.29	2.62	0.38
Dikson	Russia	1950–1997	80.4	73.5	0.19	0.5	1.55	/
Uedinenia	Russia	1953–1995	82.2	77.5	−1.91	0.56	2.11	/
Izvestia Tsik	Russia	1954–2009	82.95	75.95	−0.58	0.3	3.04	2.83
Sterlegova	Russia	1950–1995	88.9	75.417	−0.51	0.55	2.14	/
Isachenko	Russia	1954–1993	89.2	77.15	−1.58	0.65	4.49	/
Golomianyi	Russia	1954–2009	90.617	79.55	−1.61	0.41	0.36	0.58
Pravdy	Russia	1950–1994	94.767	76.267	−1.01	0.52	3.24	/
Russkii	Russia	1951–1989	96.433	77.167	−1.24	0.28	2.61	/
Krasnoflotskie	Russia	1954–1987	98.833	78.6	−0.95	0.04	3.05	/
Geiberga	Russia	1951–1995	101.517	77.6	−0.78	0.55	2.83	/
Peschanyi	Russia	1962–1993	102.483	79.433	−0.22	0.67	3.59	/
Fedorova	Russia	1950–2000	104.3	77.717	−0.47	0.3	1.84	/
Malyi	Russia	1950–1991	106.817	78.083	−0.16	0.43	2.43	/
Andreia	Russia	1951–1999	110.75	76.8	−0.12	0.54	3.3	/
Preobrazhenia	Russia	1951–1991	112.933	74.667	−0.39	0.41	0.45	/
Terpiai	Russia	1956–1998	118.667	73.55	−0.5	0.5	2.24	/
Dunai	Russia	1951–2009	124.5	73.933	−0.46	0.26	2.56	12.52
Tiksi	Russia	1950–2009	128.917	71.583	−0.58	0.27	2.06	6.08
Muostah	Russia	1951–1995	130.033	71.55	−0.58	0.41	3.03	/
Sannikova	Russia	1950–2009	138.9	74.667	−0.49	0.19	1.74	5.01
Kigiliah	Russia	1951–2009	139.867	73.333	−0.55	0.15	0.95	3.32
Sviatoi	Russia	1951–1987	140.733	72.833	−0.56	−0.35	3	/
Zemlia	Russia	1951–1987	142.117	74.883	−0.48	−0.6	3.78	/
Shalaurova	Russia	1950–2001	143.233	73.183	−0.55	0.01	1.18	/
Zhohova	Russia	1950–2000	152.833	76.15	−0.14	0.29	1.91	/
Ambarchik	Russia	1950–1995	162.3	69.617	−0.47	−0.02	3.63	/
Chetyrehstolbovoi	Russia	1951–1994	162.483	70.633	−0.4	−0.03	1.73	/
Rau-Chua	Russia	1950–1989	166.583	69.5	−0.42	−0.04	0.73	/
Aion	Russia	1954–2001	167.983	69.933	−0.36	0.08	0.96	/
Pevek	Russia	1950–2009	170.25	69.7	−0.35	0.07	3.66	8.77
Valkarkai	Russia	1956–1993	170.933	70.083	−0.3	0.15	3.46	/
Billinga	Russia	1953–1995	175.767	69.883	−0.21	0.07	1.92	/
Mys Shmidta	Russia	1950–1994	180.633	68.9	−0.13	0.03	1.86	/
Vrangelia	Russia	1950–2000	181.517	70.983	0.19	0.08	2.32	/
Vankarem	Russia	1950–2002	184.167	67.833	−0.06	0.14	2.78	/
Koluchin	Russia	1950–1991	185.35	67.483	−0.04	0.17	2.54	/
Netten	Russia	1950–1995	188.067	66.967	0.07	0.08	1.92	/

CMSL trend over 1980–2009 amounts to 2.25 +/− 0.26 mm/yr. The latter value compares well with the global mean sea level trend over the same time span (1980–2009) (equal to 2.09 +/− 0.04 mm/yr [*Church and White*, 2011]). On average over the whole 60-year time span (1950–2009), we find a positive Arctic CMSL trend of 1.62 +/− 0.11 mm/yr (after correcting for GIA and IB). For the Russian sector alone, *Proshutinsky et al.* [2004] found a rate of sea level rise of about 1.3 mm/yr over 1954–1989 after correcting for GIA and IB. Over the same time span (1954–1989), our Arctic CMSL trend amounts to 1.70 +/− 0.24 mm/yr. This trend is slightly larger than *Proshutinsky et al.*'s [2004] value, but refers to both Russian and Norwegian coasts.

[19] Considering only the 27 time series of data set1 to construct Arctic CMSL (not shown) gives the same result. Again Arctic CMSL rate is quite similar to the global mean rate over 1950–2009 (1.8 +/− 0.15 mm/yr [*Church and White*, 2011]). Thus so far, Arctic CMSL does not seem to rise faster than the global mean sea level.

[20] As indicated above, strong interannual variability affects Arctic CMSL. On Figure 6, we superimposed the Arctic Oscillation (AO) index to the CMSL curve. The AO is an important climate index of the Arctic region, referring to opposing atmospheric pressure patterns in northern middle and high latitudes. It exhibits a negative phase with

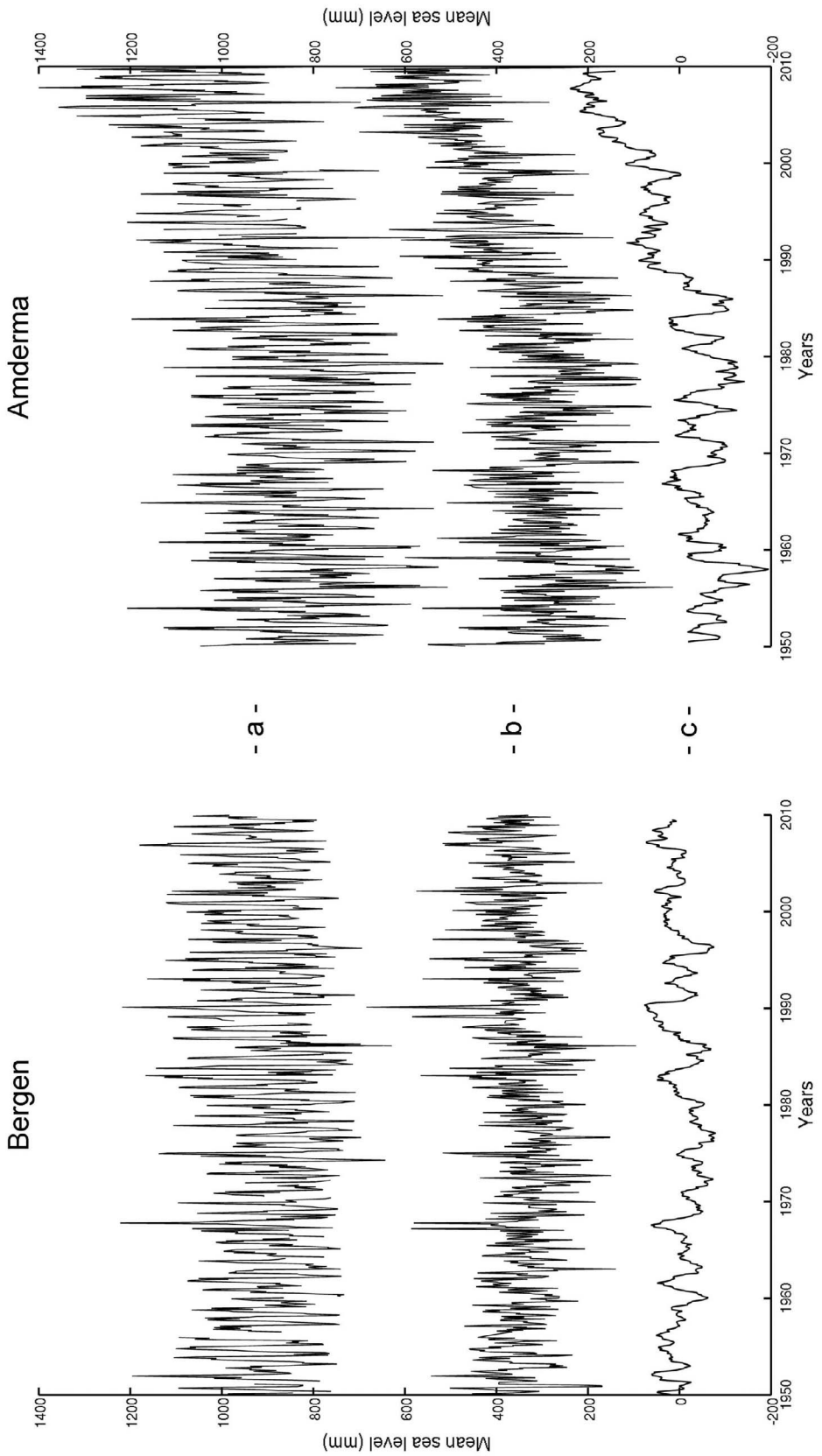

Figure 2. Tide gauge time series at Bergen (Norway) and Amderma (Russia): (a) raw data, (b) raw data minus the 12-month and 6-month sinusoids, and (c) smoothed data (12-month running mean smoothing applied to the middle curve).

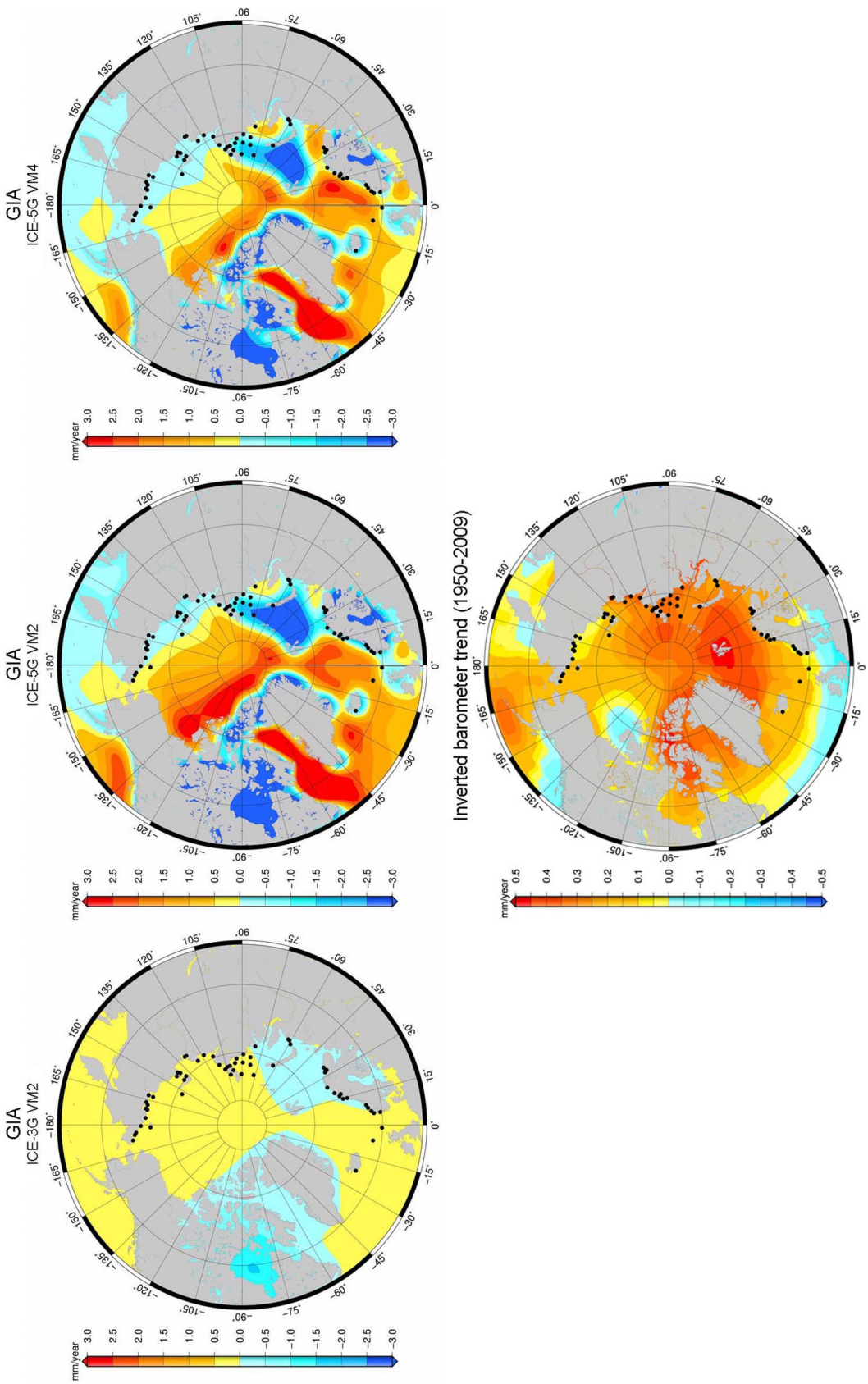

Figure 3. Regional GIA rates (mm/yr) for the ICE-3G/VM2 and ICE-5G-VM2/VM4 models, and IB (inverted barometer) trends over 1950–2009 (mm/yr). Black dots represent the tide gauge sites used in this study.

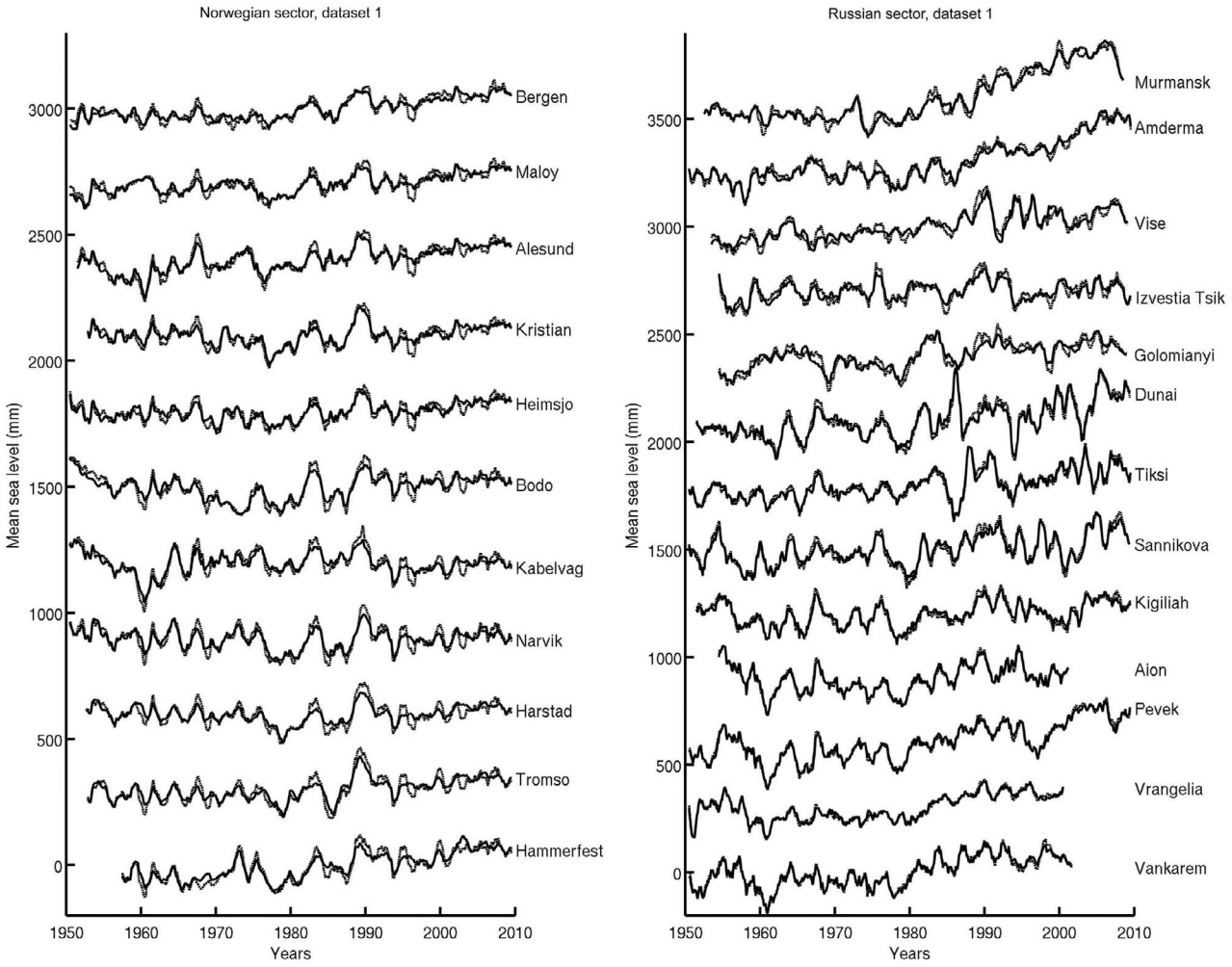

Figure 4. Plots of individual tide gauge time series with (solid line) and without (dashed line) the IB correction over 1950–2009 for the (left) Norwegian sector (11 tide gauges) and (right) Russian sector (13 tide gauges).

relatively high pressure over the polar region and low pressure at midlatitudes, and a positive phase during which the pattern is reversed. Over most of the past century, the AO alternated between its positive and negative phases. Starting in the 1970s, however, the oscillation has tended to stay in the positive phase, with strong positive values in the early 1990s. During the past decade, the AO has been low and much variable. A number of previous studies reported that several meteorological and climatic variables of the Arctic region are highly correlated with the AO index (and with the North Atlantic Oscillation -NAO- [e.g., *Chylek et al.*, 2010]).

[21] Looking at Figure 6, we indeed observe significant correlation between Arctic CMSL curve and AO up to 1995–2000. Most of the large interannual oscillations seen in the CMSL curve, in particular the high positive anomaly in the early 1990s, are also visible in the AO index. The correlation, between 1950 and 1995, amounts to 0.68 (95% confidence). However, surprisingly, beyond the mid-1990s and especially since 2000, the correlation breaks down, even if at interannual time scale, there is still some agreement between the two curves. The Arctic CMSL shows sustained rise since about 1995 while the AO index does not, oscillating between positive and negative values. We performed tests with other climate indices such the NAO but the correlation between CMSL and AO was found higher.

[22] It seems surprising at first look to find a significant correlation between AO and IB-corrected CMSL because AO is purely sea level pressure-based parameter. However, AO also reflects large-scale atmospheric forcing and is a measure of the polar vortex, which defines changes in wind stress and wind direction that may influence the ocean circulation, hence sea level. So far we have just corrected for the purely static IB effect. The observed correlation thus suggests that other factors (e.g., wind stress and associated circulation changes, and ocean mass changes due to land ice melt and possibly river runoff) contribute to the year-to-year variability in CMSL.

[23] The above results indicate that between 1950 and the mid-to-late 1990s, Arctic CMSL was mostly driven by internal climate modes, in particular the AO, possibly through changes in wind stress and associated ocean circulation (although quantitative analyses of the latter effects

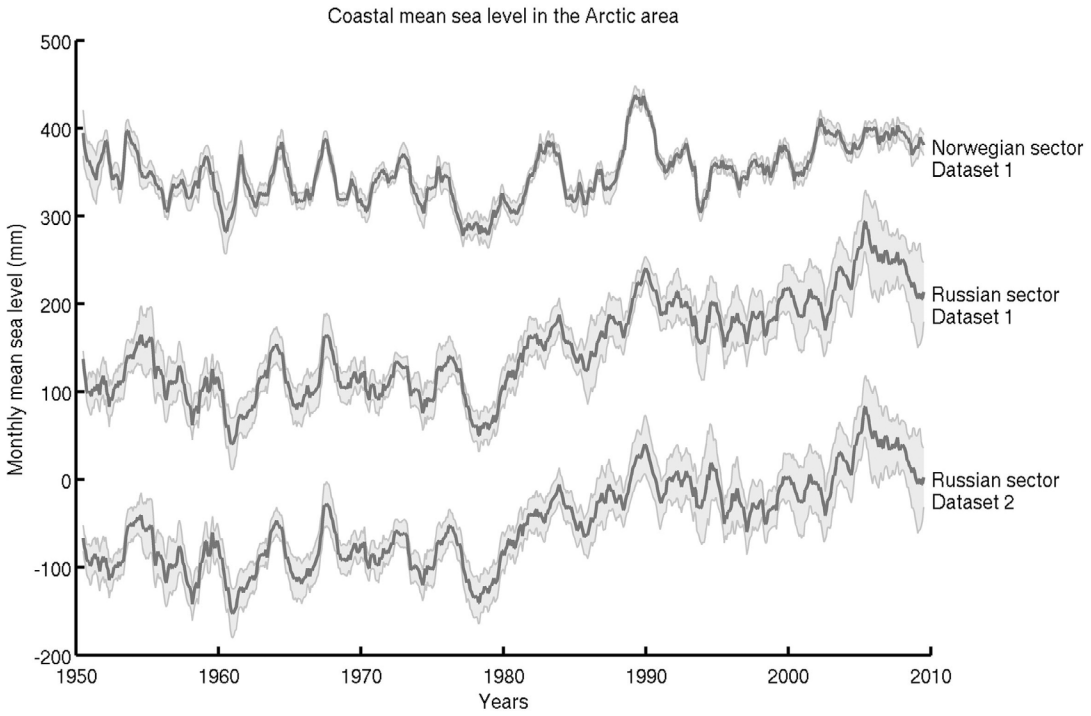

Figure 5. CMSL curves in the Norwegian (data set1) and Russian sectors (data set1 and 2). The light gray zone represents the uncertainty of the CMSL time series.

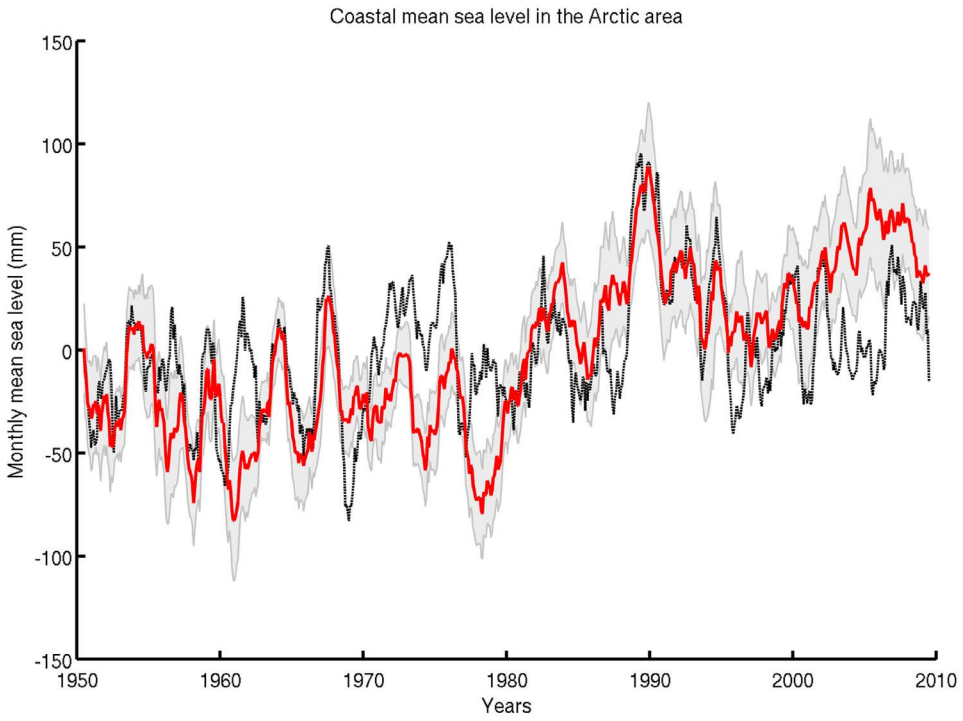

Figure 6. Arctic CMSL curve (red solid curve) and associated uncertainty (light gray zone). Arctic oscillation index is superimposed (black dashed curve).

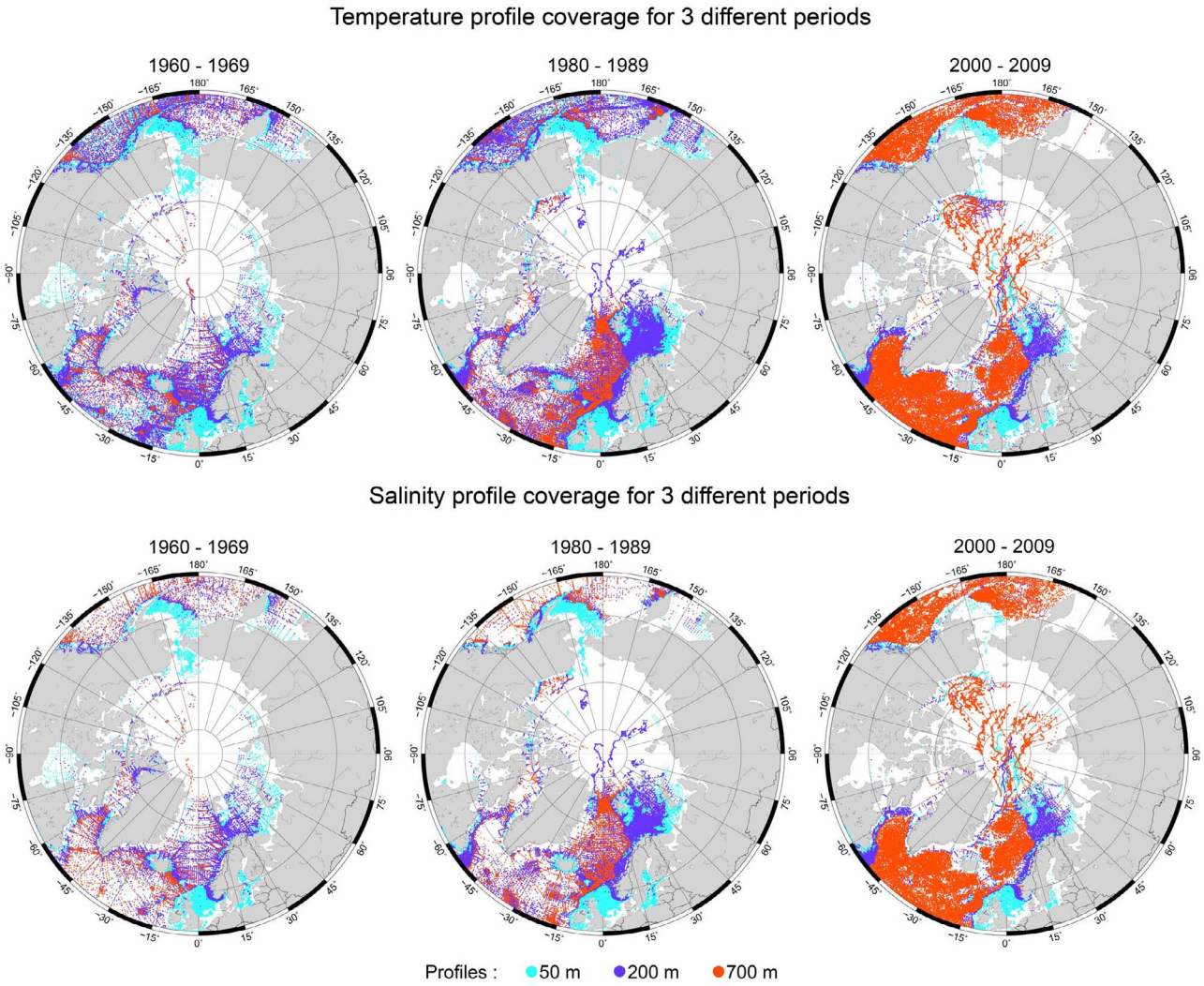

Figure 7. (top) Temperature and (bottom) salinity profile coverage (data from EN3) in the Arctic region for 3 different depth ranges (0–50 m, 0–200 m and 0–700 m) and 3 different periods (1960–1969, 1980–1989 and 2000–2009).

remain to be performed), as well as ocean mass changes. Since the mid-to-late 1990s, Arctic CMSL shows a marked rise of 4.07 +/− 0.65 mm/yr.

4. Steric Sea Level in the North Atlantic and Nordic Seas

4.1. Steric Data

[24] In this section we estimate the contribution of the steric (effect of ocean temperature T (thermosteric component) and salinity S (halosteric component)) sea level to Arctic CMSL. For that purpose, we use T/S data from 3 different databases: the WOD09 [*Levitus et al.*, 2009], the *Ishii and Kimoto* [2009] (called IK09 hereafter) databases and the EN3 database developed by the Met Office/Hadley Centre, UK [*Ingleby and Huddleston*, 2007]. The EN3 database consists of the WOD05 database [*Levitus et al.*, 2005] plus additional T data from the ASBO (Arctic Synoptic Basin-wide Oceanography) project (see NOCS ASBO web page: http://www.noc.soton.ac.uk/ooc/ASBO/index.php) and Argo project. The WOD09 and IK09 databases account for depth-bias corrections on XBT temperature data [e.g., *Wijffels et al.*, 2008], unlike the WOD05 data included in the EN3 gridded database (after this study was started, XBT depth bias corrections were posted along T profiles on the EN3 web site; however, accounting for profile-based depth bias corrections was found beyond the scope of the present study; nevertheless the EN3 database include a large portion of non XBT data which do not suffer from XBT depth-bias). The T/S data from the 3 databases are publicly available at: http://www.nodc.noaa.gov/OC5/indprod.html for WOD09; http://atm-phys.nies.go.jp/~ism/pub/ProjD/v6.9/ for IK09; and http://www.metoffice.gov.uk/hadobs/en3/index.html for EN3.

[25] The depth and time coverage of these data is very inhomogeneous in the studied region, leaving much of the Arctic Ocean uncovered. This is illustrated in Figure 7 which shows for three periods (1960–1969, 1980–1989 and 2000–2009) T and S data coverage (from EN3) down to 700 m (coverage is shown for the 0–50 m, 0–200 m and 0–700 m upper ocean layers). The coverage during the 1960s and

earlier is far too sparse and limited to the near surface layers, preventing us to quantify the steric contribution in the whole Arctic and even along the Russian coasts. Before the 1990s, we also note that the data coverage is poor. This leads us to not consider data prior to 1970 and only consider a limited geographical sector bounded by the 75°W–45°E longitudes and the 50°N–80°N parallels.

4.2. Steric Spatial Trend Patterns

[26] For each database, we computed the thermosteric sea level on a 1° × 1° grid at monthly interval since 1970 (at 3-month intervals for WOD09), integrating T anomalies from the surface down to 700 m. For that purpose, we first computed density anomalies at each standard level down to 700 m by considering temperature anomalies and using the classical equation of state of the ocean. Then, we integrated density anomalies at each grid point (using a climatology for the salinity) and each time step to obtain the thermosteric sea level [*Gill*, 1982; *Levitus et al.*, 2005; *Lombard et al.*, 2005].

[27] We also computed the halosteric sea level using salinity anomalies available for the IK09 and EN3 databases (no gridded salinity data are available for WOD09). We followed the same methodology as for the thermosteric sea level but now considering salinity anomalies from the surface down to 700 m and a climatology for the temperature.

[28] Figures 8a and 8c show thermosteric trend patterns computed over 1970–2009 for the IK09 and WOD09 data over the limited region described above. We note that thermosteric spatial trends are positive almost everywhere and very similar in both cases, with higher rates than average south of Iceland, in the Baffin Bay, Greenland and Norwegian seas. Figure 8b shows halosteric spatial trend patterns for IK09. Halosteric trends are moderately negative over the studied area, indicating a slight increase in salinity since 1970. Comparing thermosteric and halosteric trend maps for IK09 shows that the patterns are anticorrelated (with higher magnitude for the thermosteric trends). This anticorrelation between thermosteric and halosteric trend patterns suggests simultaneous increase of both temperature and salinity since 1970 in the North Atlantic and Nordic Seas sector (the two factors having opposite effects on sea level). A similar behavior has been reported in several other regions from in situ hydrographic data and/or ocean circulation modeling [e.g., *Wunsch et al.*, 2007; *Köhl and Stammer*, 2008].

[29] Figure 9 shows the steric (sum of thermosteric and halosteric) trend patterns over 1970–2009 for the IK09 and EN3 data (note that computing the steric sea level by summing the thermosteric and halosteric components or by direct integration of T- and S-related density anomalies gives essentially the same result). The two maps show more or less similar patterns in the North Atlantic and Nordic Seas, in particular along the Norwegian coast. Some difference is noticed however in the Baffin Bay and southwest of Greenland.

4.3. Interannual Variability of the Gridded Steric Data

[30] To investigate the dominant modes of variability of the steric data in the limited region considered above, we performed an EOF (empirical orthogonal function) decomposition [*Preisendorfer*, 1988] of the WOD09 and IK09 gridded thermosteric data over the 1970–2009 time span. Figure 10 (top) shows corresponding first spatial and temporal mode (noted EOF1) for the two thermosteric data. We note that EOF1s (42.9 and 46.1% of the total variance, respectively) are highly correlated both spatially and temporally, and closely resemble the thermosteric trend patterns shown in Figure 8. The temporal curves are also highly correlated. They are flat until 1995 but since then show an upward trend. Figure 10 (bottom) shows EOF1 of IK09 halosteric data decomposition. The anticorrelation noted above for the spatial trend patterns between thermosteric and halosteric components is even more evident in EOF1s. Like EOF1 thermosteric temporal curve, the EOF1 halosteric temporal curve also displays an upward trend as of 1995 (associated with negative spatial trend values), suggesting simultaneous increase of temperature and salinity in the region. To see more clearly the latter behavior, we have averaged the gridded thermosteric (IK09 and WOD09) and halosteric (IK09) data at each time step over the region, and computed the mean thermosteric and halosteric curves. These are shown in Figure 11. We first note that the two thermosteric curves agree well. We also note the strong change and opposite behavior affecting the thermosteric and halosteric curves as of ∼1995.

4.4. Steric Sea Level at the Norwegian Tide Gauges

[31] We computed the steric sea level (thermosteric plus halosteric components) using the IK09 and EN3 data since 1970 at the 11 Norwegian tide gauge sites by interpolating the steric grids at the tide gauge locations (averaging the gridded data within a 1° radius around the tide gauge). Corresponding curves are shown in Figure 12 (top) superimposed to the Norwegian CMSL curve. We first note that both IK09 and EN3 curves are in general good agreement (as previously noticed between IK09 and WOD09 thermosteric components). Although smoother, they correlate also well between 1970 and 2006 with the CMSL curve (correlation of 0.65). However, as of 2006, the steric sea level curves show a downward trend not seen in the CMSL curve. The steric sea level trends over 1970–2006 amounts to 1.63 +/− 0.14 mm/yr and 1.9 +/− 0.17 mm/yr for IK09 and EN3 respectively, a value quite comparable to the CMSL trend over the same time span (of 1.73 +/− 0.23 mm/yr). This suggests that, at least over this time span (1970–2006), observed CMSL rise along the Norwegian coast has a steric origin. However, the interannual variability in steric sea level and Norwegian CMSL are not well correlated, suggesting that the latter is influenced by other factors on such time scales, e.g., wind stress-driven ocean circulation and ocean mass changes.

[32] We computed the residual (observed CMSL minus steric sea level) curve at the Norwegian tide gauges with the IK09 and EN3 data. The corresponding time series over 1970–2006 are shown in Figure 12 (bottom). The AO index is superimposed. The trend of the residual curves over 1970–2006 amount to 0.11 +/− 0.23 mm/yr and −0.17 +/− 0.22 mm/yr for the IK09 and EN3 data, respectively, thus are not significant. On the other hand, the residual curves show important interannual variability moderately correlated with the AO index. Over 1970–2006, this correlation is equal to 0.54 only but at some periods (e.g., around 1990), the sea level residuals and the AO co-vary similarly, possibly reflecting the dynamical response of the sea to wind-forcing. At the end of the studied period (around 2006), the residual curves show an upward trend not seen on

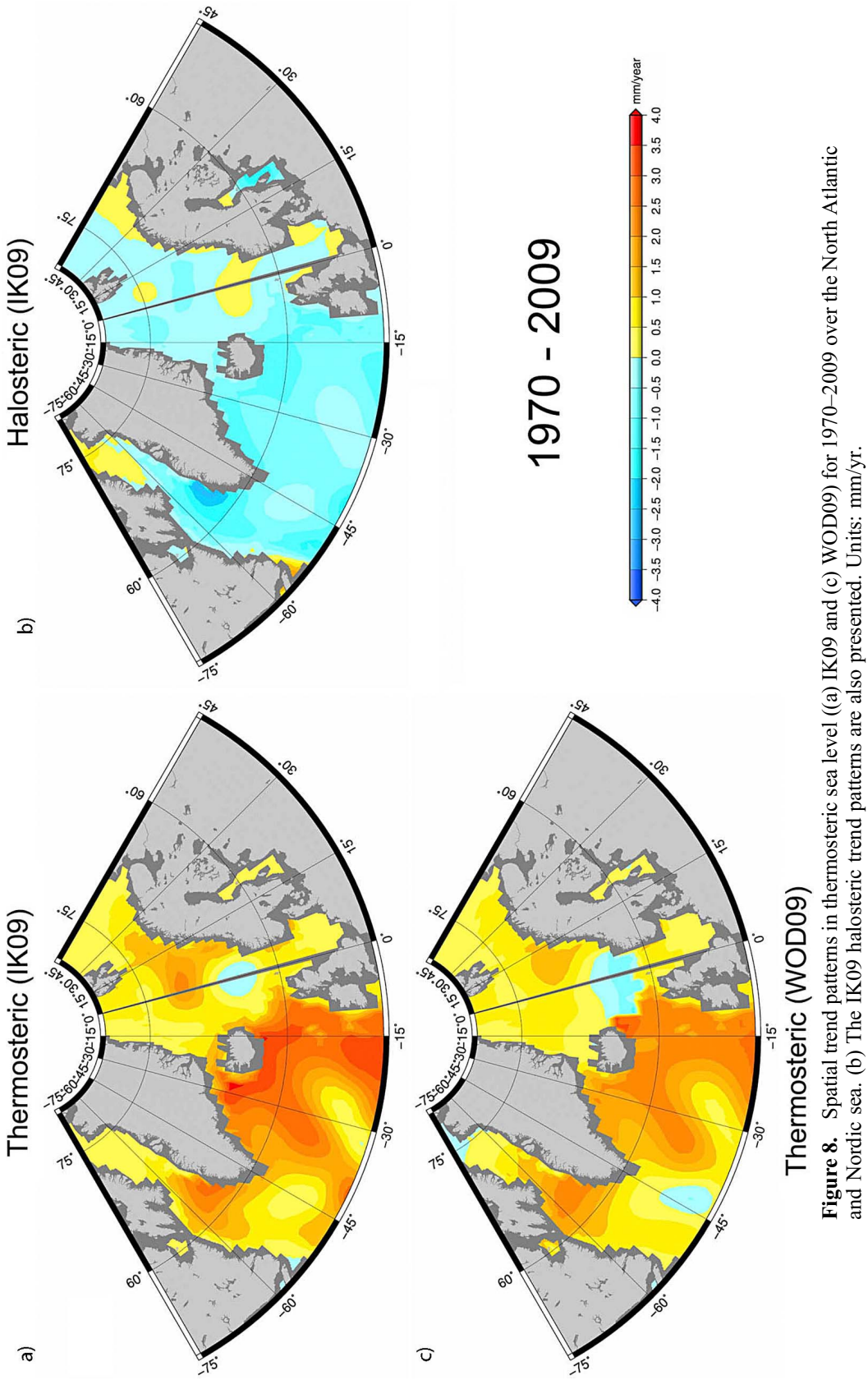

Figure 8. Spatial trend patterns in thermosteric sea level ((a) IK09 and (c) WOD09) for 1970–2009 over the North Atlantic and Nordic sea. (b) The IK09 halosteric trend patterns are also presented. Units: mm/yr.

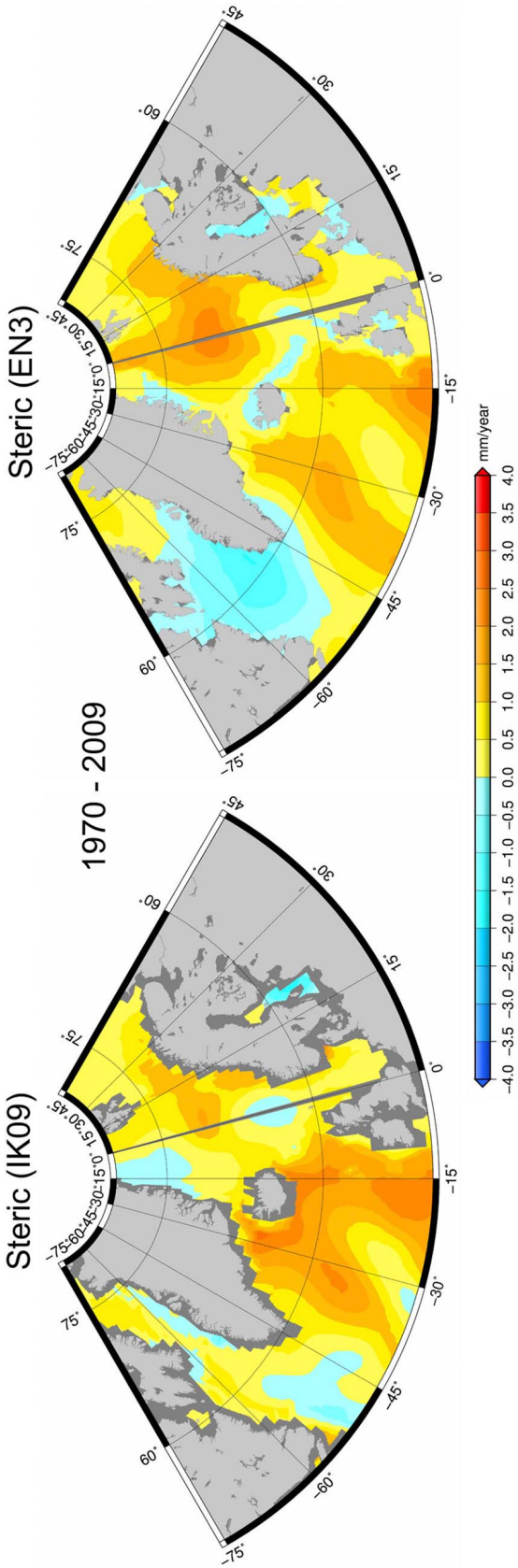

Figure 9. Spatial trend patterns in steric sea level for (left) IK09 and (right) EN3 data for 1970–2009. Units: mm/yr.

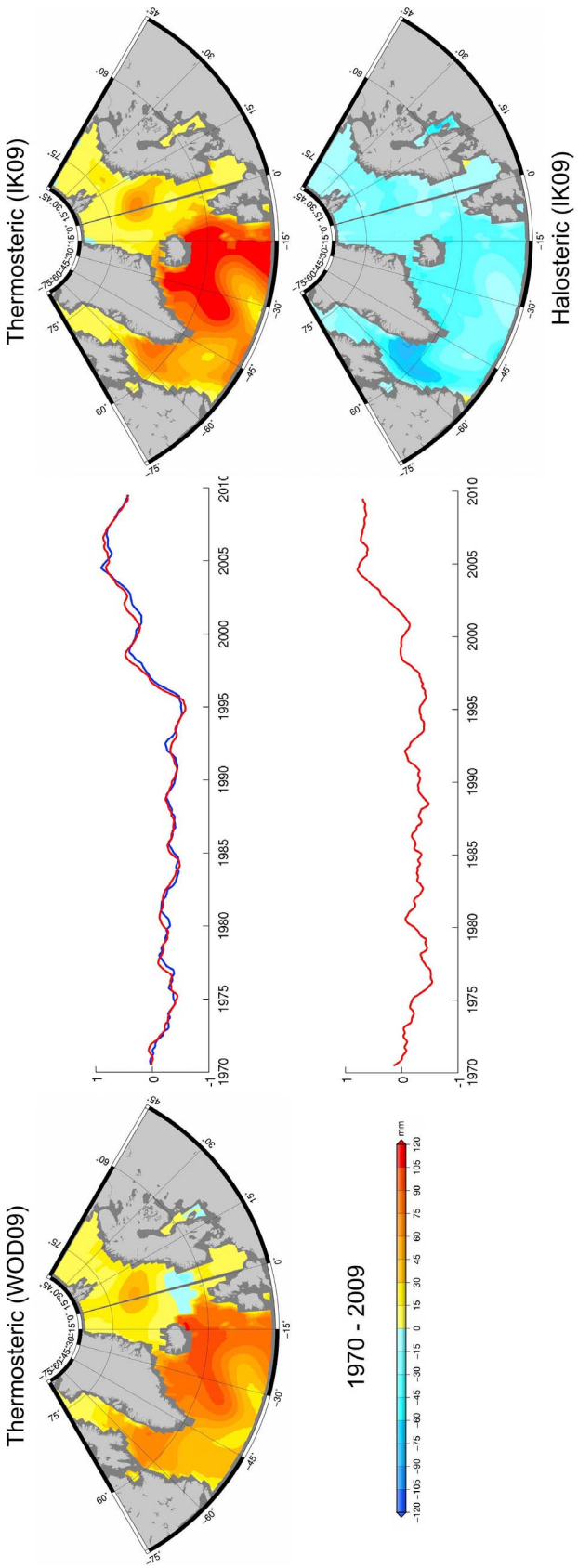

Figure 10. (top) EOF mode 1 of thermosteric sea level for WOD09 (red curve) and IK09 (blue curve) over 1970–2009. (bottom) EOF mode 1 of IK09 halosteric sea level.

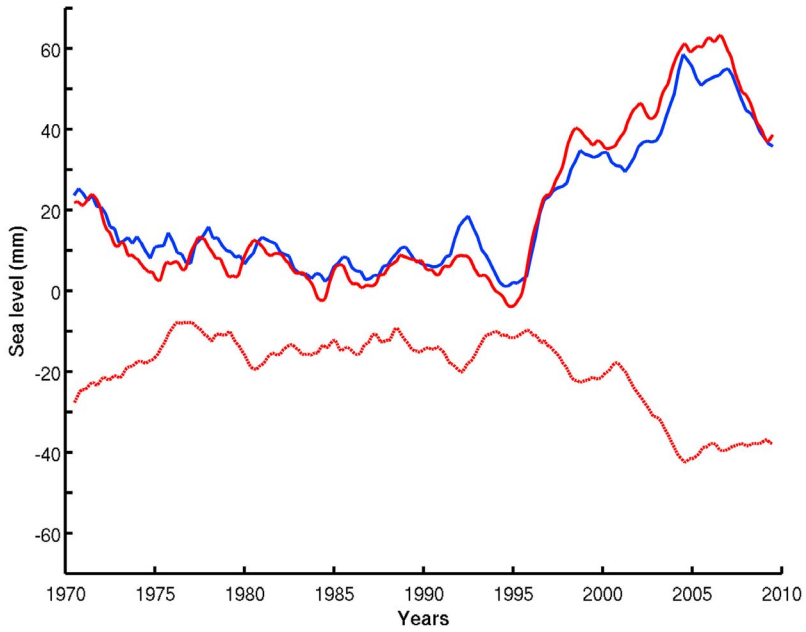

Figure 11. Top curves are regionally averaged thermosteric sea level over 1970–2009 (region as shown in Figures 8 and 9) for IK09 (red curve) and WOD09 (blue curve) data. Bottom curve is regionally averaged halosteric sea level (IK09 data, red curve).

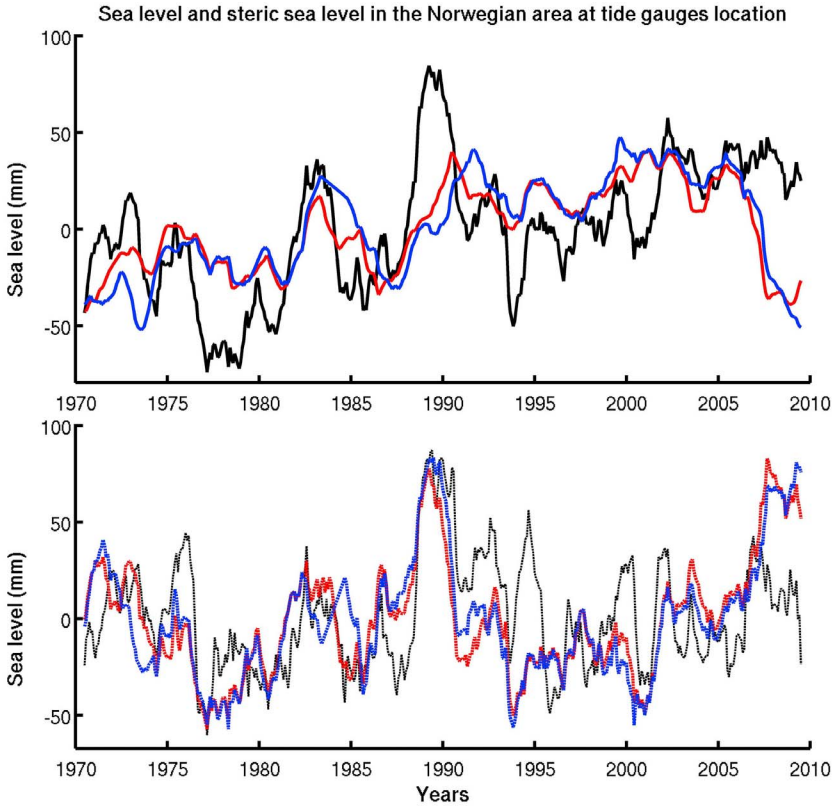

Figure 12. (top) CMSL at the Norwegian tide gauges (black curve) over 1970–2009 on which is superimposed the steric sea level (IK09: red curve and EN3: blue curve) interpolated at the tide gauge sites. (bottom) Residual (observed minus steric) sea level (red and blue curves for IK09 and EN3 respectively). The AO index is superimposed (black-dashed curve).

the AO. This may reveal an increased contribution of the ocean mass component linked to the recently reported acceleration in land ice melt [i.e., *Holland et al.*, 2008; *Steffen et al.*, 2010; *Rignot et al.*, 2011] plus regional water mass redistribution. We will come back to this issue in section 5.

5. Comparison Between Tide Gauge-Based, Altimetry-Based and Steric Sea Level in the North Atlantic and Nordic Seas Over 1993–2009 and Estimate of GRACE-Based Ocean Mass Over 2003–2009

[33] In this section, we take advantage of the availability of gridded altimetry sea level data up to 82°N since 1993 to investigate in more detail the mean and regional sea level in the North Atlantic and Nordic Seas sector and its relationship with the steric sea level. Satellite altimetry measures absolute sea level (i.e., relative to the Earth's center of mass [*Fu and Cazenave*, 2001; *Cazenave and Nerem*, 2004]), thus reflects global/regional changes in ocean water volume (due to density changes and water mass variations) as well as additional factors causing regional variability in sea level such as the deformations of ocean basins in response to land ice melt-induced mass redistribution [*Milne et al.*, 2009; *Tamisiea and Mitrovica*, 2011]. As altimetry-based sea level does not sense vertical crustal motions, it can be compared to tide gauge-based sea level, once the latter is corrected for vertical crustal motions. Here we use the multi mission altimetry data reprocessed by *Prandi et al.* [2012]. This reprocessing improves the data coverage and the quality of the geophysical corrections to apply to the altimetry data in the Arctic region. The details of the data reprocessing is described in *Prandi et al.* [2012]. The inverted barometer correction is applied to altimetry data as for the tide gauge data using the *Carrère and Lyard* [2003] model.

5.1. Spatial Trend Patterns in Altimetry-Based and Steric Sea Level (1993–2009)

[34] We compared the altimetry-based sea level trend patterns with the thermosteric and halosteric spatial patterns (IK09 data) for the 1993–2009 time span over the North Atlantic and Nordic Seas sector. These are shown in Figures 13a–13c. In several areas, e.g., south of Iceland and Greenland and in the Norwegian Sea, the spatial trend patterns of altimetry-based and thermosteric sea level show positive trends. Thermosteric trends have larger amplitude than observed (i.e., altimetry-based) ones, but because of opposite trends in the halosteric component (see Figures 13a–13c), their sum (i.e., the steric component) will better agree with altimetry-based trends. This is indeed the case (although not everywhere), as illustrated in Figures 13d and 13e showing steric trend patterns over 1993–2009 for the IK09 and EN3 data.

[35] We computed residual trend maps (i.e., altimetry-based minus steric trends) with the IK09 and EN3 data over 1993–2009. These are shown in Figure 14. In most areas (northwest and southeast of Greenland, Greenland and Norwegian seas, and along the coasts of Norway), the residual trend patterns roughly agree. Although part of the residual trends may result from uncertainty and imperfect data coverage of T/S data in the region, we cannot exclude that they reflect real non-steric signals, for example ocean mass changes. Since ~2003, the latter are measurable by GRACE space gravimetry data. This is discussed in the next section.

5.2. Tide Gauge-Based, Altimetry-Based, GRACE-Ocean Mass and Steric Sea Level Along the Norwegian Coasts

[36] We interpolated the altimetric grids at the tide gauge locations (as done for the steric sea level in section 4). At the Norwegian tide gauges, the altimetry-based and tide gauge-based sea level time series are highly correlated both in terms of trend and interannual variability, with all correlations >0.9 (not shown). The highest correlation was obtained when the ICE-5G/VM2 GIA correction was used for the tide gauge data. This was the basis for preferring this particular GIA correction (see section 3). We constructed an altimetry-based CMSL along the Norwegian coast averaging individual time series at the 11 tide gauge sites of data set1. The tide gauge and altimetry-based CMSL curves in the Norwegian sector for 1993–2009 are shown in Figure 15 (top). Both curves are highly correlated and show an increasing sea level trend of 3.32 +/− 0.65 mm/yr (from tide gauges) and 4.23 +/− 0.23 mm/yr (from satellite altimetry) over the altimetry period (1993–2009). The trend difference (0.9 mm/yr) is only slightly larger than the tide gauge trend uncertainty. Thus the altimetry data clearly confirm the recent sea level increase in that particular region. We note in passing that the rate of sea level rise in this region is very similar to the global mean rate (of 3.3 mm/yr over 1993–2009 [e.g., *Cazenave and Llovel*, 2010]), a result confirmed by *Prandi et al.* [2012] for the whole Arctic region.

[37] We estimated the ocean mass change along the Norwegian coast as of 2003 using GRACE space gravimetry data [*Wahr et al.*, 2004]. GRACE measures temporal variations of the Earth's gravity field and, over the oceanic domain, provides an estimate of ocean mass changes. Several GRACE products have been released from teams involved in the GRACE project (CSR, JPL and GFZ), each time with substantial improvement [*Chambers*, 2006]. Here we use the CSR 1° × 1° gridded data over the ocean (RL04 release) at monthly interval (available at http://grace.jpl.nasa.gov/data/GRACEMONTHLYMASSGRIDSOCEAN/). These data include an implementation of the carefully calibrated combination of de-stripping and smoothing, with different half-width Gaussian filters (the solutions need to be smoothed because errors increase with wavelength). These gridded ocean GRACE products are corrected for Glacial Isostatic Adjustment using the *Paulson et al.*'s [2007] model. The data used in this study cover the time span from January 2003 to December 2009 and are expressed in sea level equivalent.

[38] We interpolated monthly GRACE-ocean mass grids at the 11 Norwegian tide gauge sites, removed the seasonal signal as for the other data sets and then averaged the 11 individual ocean mass time series. Corresponding GRACE-based averaged ocean mass curve is superimposed to the CMSL curve in Figure 15 (top). Over 2003–2009, the GRACE ocean mass trend is positive and equal to 2.9 +/− 0.66 mm/yr. This is significantly different from the CMSL trend over the same time span (equal to −1.14 +/− 0.21 mm/yr). As the CMSL trend reflects primarily the sum of the steric plus ocean mass trends, this trend difference is not really surprising considering the downward trend seen in the mean

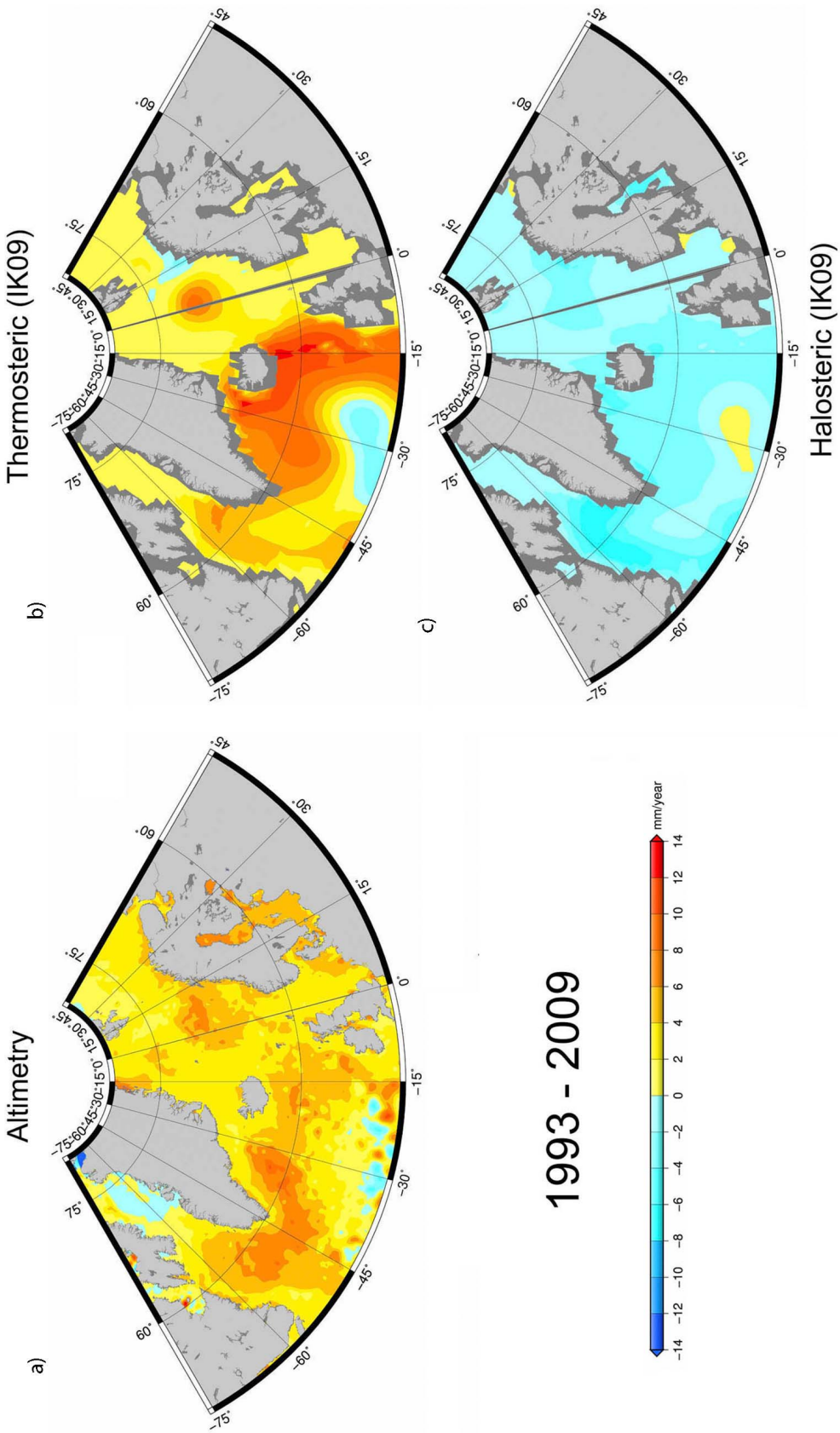

Figure 13. (a) Spatial trend patterns of altimetry-based, (b) thermosteric (IK09), and (c) halosteric (IK09) in the North Atlantic and Nordic Seas region over 1993–2009. Spatial trend patterns in steric sea level over 1993–2009 ((d) IK09 and (e) EN3). Units: mm/yr.

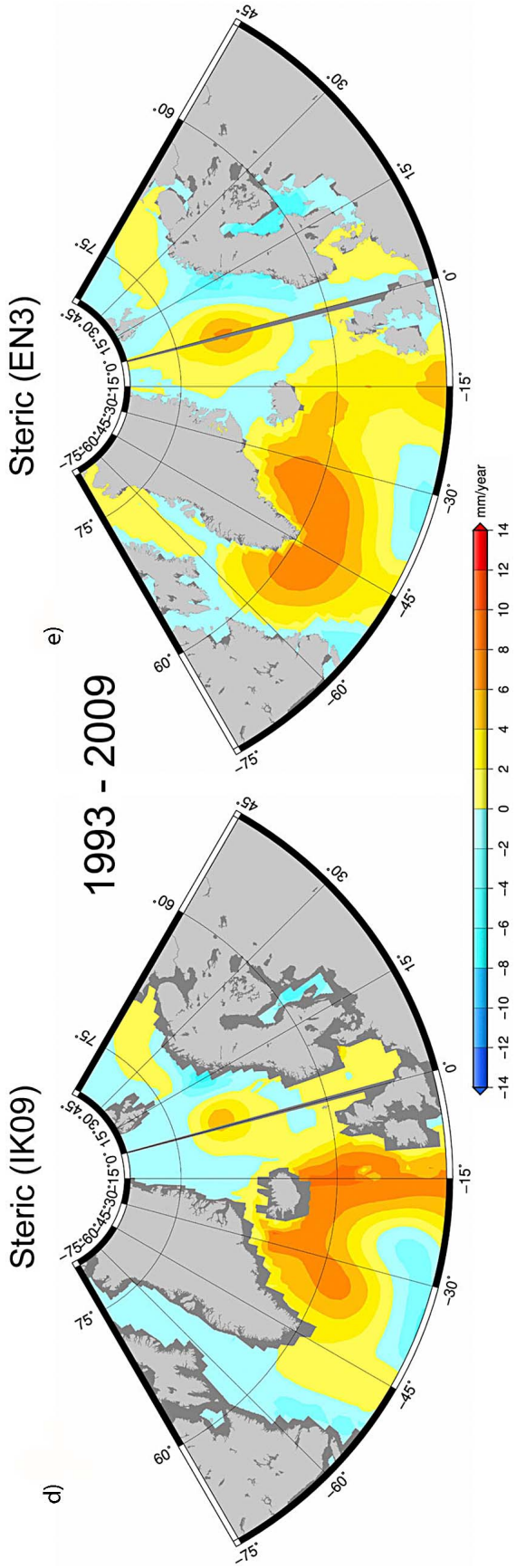

Figure 13. (continued)

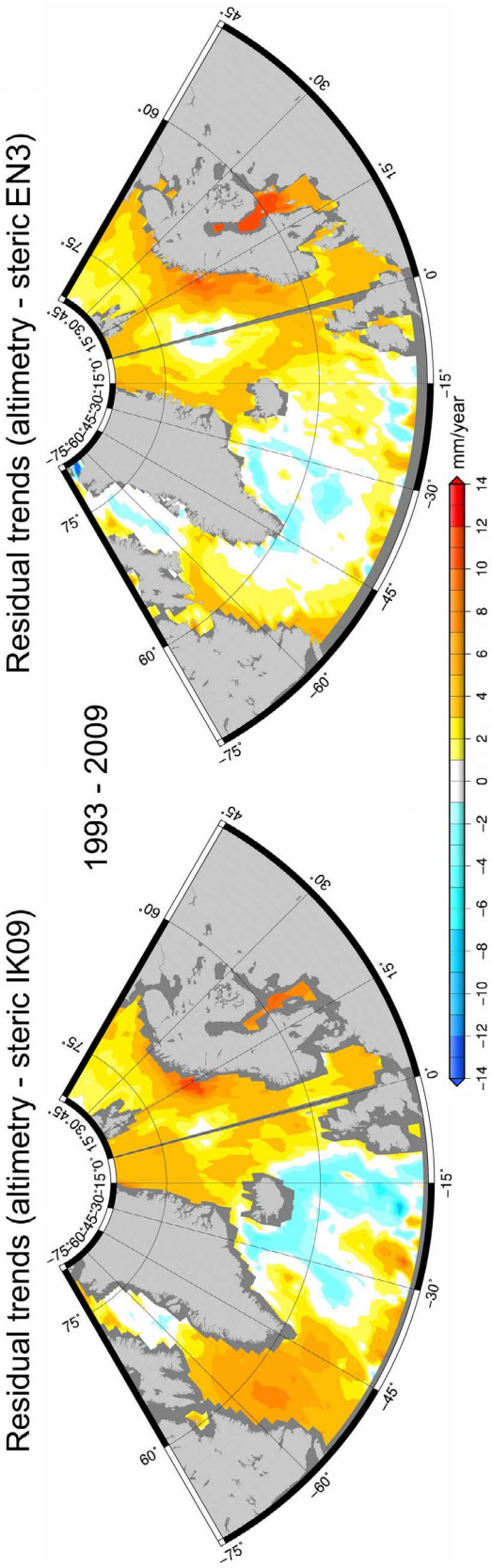

Figure 14. Spatial trend patterns of the residual (altimetric minus steric) sea level in the North Atlantic and Nordic Seas region over 1993–2009 ((left) IK09 and (right) EN3). Units: mm/yr.

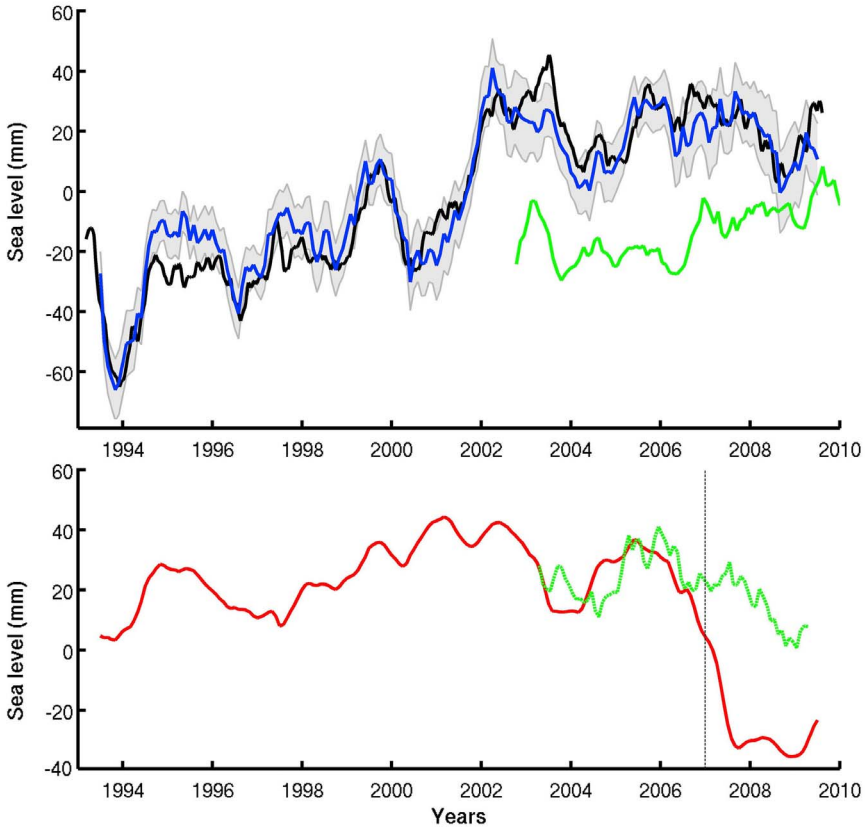

Figure 15. (top) Tide gauge-based (blue curve) and altimetry-based CMSL (black curve) at the Norwegian tide gauge sites over 1993–2009. The green curve represents the GRACE-based ocean mass component averaged at the Norwegian tide gauge sites. (bottom) Mean steric sea level (IK09 data, red curve); the green curve represents the steric component estimated from the difference between tide gauge-based CMSL and GRACE ocean mass. The dashed vertical line corresponds to the date (early 2007) beyond which no ocean temperature data are available along the Norwegian coast.

steric sea level averaged at the Norwegian tide gauges (Figure 12, top). On the other hand, reasonable agreement is observed between CMSL sea level and GRACE-based ocean mass in terms of year-to-year variability.

[39] In Figure 15 (bottom) is shown the difference over 2003–2009 between CMSL and GRACE-based ocean mass averaged at the Norwegian tide gauges. This difference should primarily reflect the steric component. The coastal steric sea level from the IK09 data is also shown over 1993–2009. While both curves show a downward trend over their overlapping time span (2003–2009), the highly negative observed steric trend seems somewhat suspect. This highly negative steric trend may not be real and may simply reflect lack of data in the very recent years. To check this, we looked at the T/S data coverage between 2005 and 2009. This is illustrated in Figure 16 showing yearly coverage in T data for years 2005 to 2009. Figure 16 clearly reveals very poor data coverage along the Norwegian coast over this time span. We note data down to 200 m only in 2005 and 2006. But in 2007, 2008 and 2009, there is no data at all along the Norwegian coast. Thus the interpolated steric curve (Figure 15, bottom) is likely biased low for these years. Besides considering the 2003–2006 time span during which there are some T data, we note that the "CMSL minus GRACE ocean mass" curve closely follows the steric curve, and both trends (equal to 1.41 +/− 0.7 mm/yr and 1.36 +/− 0.4 mm/yr for "CMSL-GRACE ocean mass" and steric sea level respectively over 2003–2006) agree quite well.

6. Discussion

[40] In this study, we estimated the mean sea level over the past ∼60 years along the Norwegian and Russian coasts using good quality tide gauge data. Between 1950 and 1980, coastal sea level did not rise significantly but beyond 1980, it shows a significant upward trend. Estimate of the thermosteric and halosteric sea level since 1970 in a limited sector including the North Atlantic subpolar gyre and the Nordic Seas indicates a strong change around 1995, with simultaneous increase in temperature and salinity. Along the Norwegian coast, a similar behavior is noticed with an increasing trend of observed sea level (from tide gauges and satellite altimetry) since the mid-1995s (note that the downward trend observed in the mean coastal steric sea level as of 2007 is likely an artifact due to a lack of data in this region over the very recent years). We also observe an increase in the GRACE-based averaged ocean mass at the Norwegian coast since 2003. Its positive trend (of 2.9 +/− 0.66 mm/yr over 2003–2009) is somewhat larger than the global mean ocean mass increase due to total land ice melt over about the same time span (of 1.5–2 mm/yr) [e.g., *Church and White*, 2011].

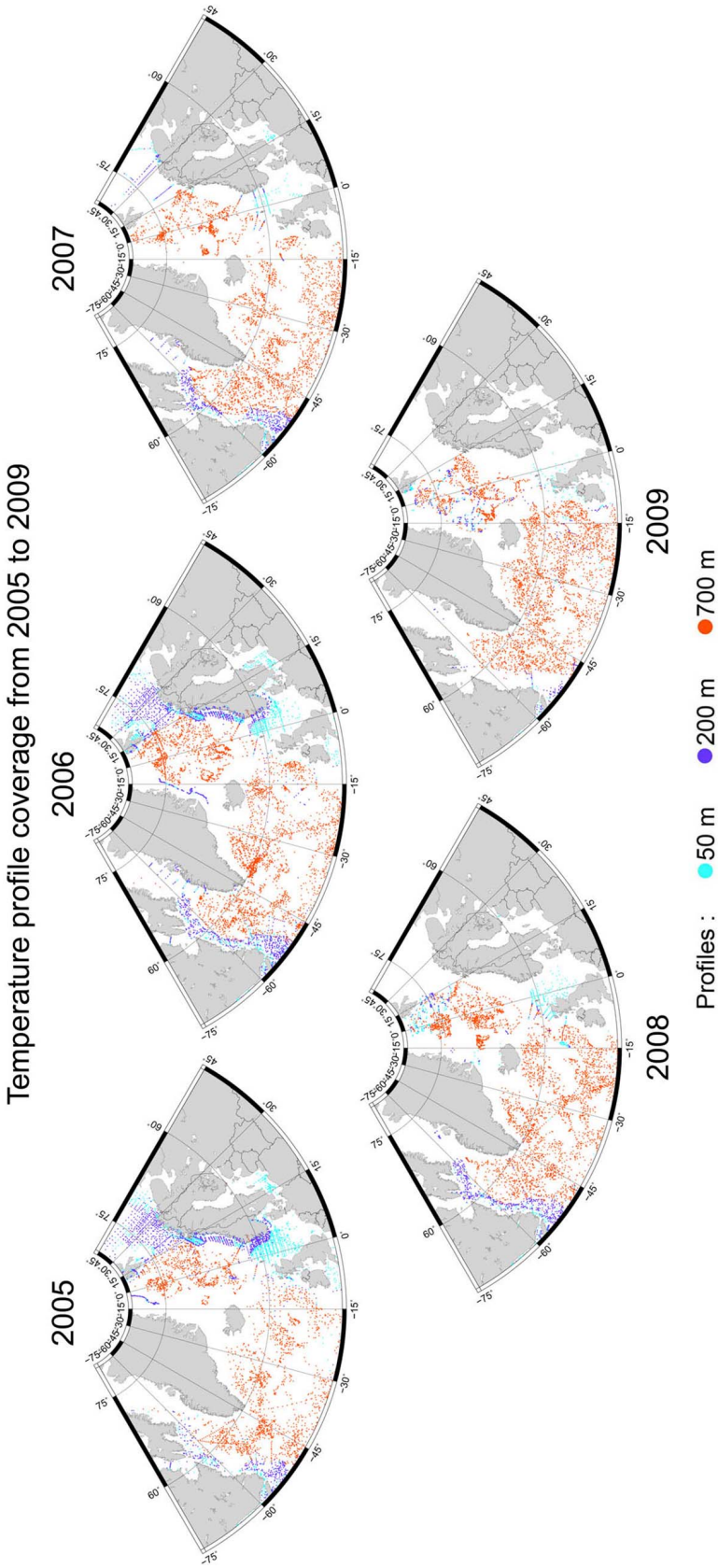

Figure 16. Temperature data coverage (EN3 data down to 700 m) for the years 2005 to 2009 in the North Atlantic and Nordic Seas sector.

It thus includes a regional ocean mass trend component (due to ocean circulation-driven mass redistribution), in addition to the global mean mass trend. Anyway, this ocean mass increase at least partly reflects the recent acceleration reported in ice mass loss from glaciers and ice sheets [e.g., *Steffen et al.*, 2010; *Rignot et al.*, 2011].

[41] The results of the present study show that between 1950 and 1995, sea level along Norwegian and Russian coasts does not display any significant upward trend, while being highly correlated to the AO. On the other hand, since the mid-to-late 1990s, coastal sea level in the Norwegian and Russian sectors has been rising faster during the previous decades. This coincides with strong changes affecting thermosteric and halosteric sea level in the North Atlantic and Nordic Seas, with simultaneous increase in temperature and salinity over the past 15 years.

[42] Recent warming of the Arctic region has been reported by *Karcher et al.* [2003] and *Polyakov et al.* [2005]. These studies observed significant changes in temperature of the Arctic and Nordic Seas during the 1990s. *Rigor and Wallace* [2004] showed that areal coverage of multiyear sea ice decreased even during 1989–1990 when the AO was in extremely high index state. This could be explained by longer ice free periods during summer, the open ocean absorbing more heat, preventing formation of sea ice (positive feedback mechanism). Warming in the Nordic Seas reduces heat loss from the Atlantic water before it enters the Arctic Ocean, with warmer Atlantic water propagating into the Arctic region. *Carton et al.* [2011] investigated the interannual/decadal variability of Atlantic water in the Nordic and adjacent seas. Their analysis shows a succession of four multiyear warm events occurring in the region between 1950 and 2009 (i.e., the same time span as in the present study), the last reported warm event began in the late 1990s and persisted for nearly a decade. Our results clearly show that in the North Atlantic, Nordic Seas and coastal zones of Norway and even Russia, significant changes also affected sea level as of mid-to-late 1990s, in agreement with other recently reported changes in Arctic climate since 1–2 decades [i.e., *Serreze and Barry*, 2011]. This period (last 15 years) may represent a transition in the Earth system evolution as recently suggested by *Peltier and Luthcke* [2009] and *Roy and Peltier* [2011]. Finally our results also show an increase of the ocean mass component along the Norwegian coast, at least partly explained by the recent acceleration in land ice loss as reported by numerous recent studies.

[43] **Acknowledgments.** This work is a contribution to the MONARCH project funded under the 7th Framework Programme of the European Union. O. Henry and P. Prandi are respectively supported by the MONARCH project and a CNES-CLS PhD grant. W. Llovel benefited of a post-doctoral NASA grant. We are very grateful to M. Ishii for useful discussions as well as to Florent Lyard for helpful exchanges about the atmospheric forcing. We thank Dick Peltier as well as the Editor of the Journal and an anonymous reviewer for their numerous and detailed comments that greatly helped us improving the manuscript.

References

Bekryaev, R. V., I. V. Polyakov, and V. A. Alexeev (2010), Role of polar amplification in long-term surface air temperature variations and modern Arctic warming, *J. Clim.*, *23*, 3888–3906, doi:10.1175/2010JCLI3297.1.

Carrère, L., and F. Lyard (2003), Modeling the barotropic response of the global ocean to atmospheric wind and pressure forcing—Comparisons with observations, *Geophys. Res. Lett.*, *30*(6), 1275, doi:10.1029/2002GL016473.

Carton, J. A., G. A. Chepurin, J. Reagan, and S. Häkkinen (2011), Interannual to decadal variability of Atlantic water in the Nordic and adjacent seas, *J. Geophys. Res.*, *116*, C11035, doi:10.1029/2011JC007102.

Cazenave, A., and W. Llovel (2010), Contemporary sea level rise, *Annu. Rev. Mar. Sci.*, *2*, 145–173, doi:10.1146/annurev-marine-120308-081105.

Cazenave, A., and R. S. Nerem (2004), Present-day sea level change: Observations and causes, *Rev. Geophys.*, *42*, RG3001, doi:10.1029/2003RG000139.

Chambers, D. P. (2006), Evaluation of new GRACE time-variable gravity data over the ocean, *Geophys. Res. Lett.*, *33*, L17603, doi:10.1029/2006GL027296.

Church, J. A., and N. J. White (2011), Sea-level rise from the late 19th to the early 21st century, *Surv. Geophys.*, *32*(4–5), 585–602, doi:10.1007/s10712-011-9119-1.

Chylek, P., C. K. Folland, G. Lesins, and M. K. Dubey (2010), Twentieth century bipolar seesaw of the Arctic and Antarctic surface air temperatures, *Geophys. Res. Lett.*, *37*, L08703, doi:10.1029/2010GL042793.

Fu, L. L., and A. Cazenave (2001), *Satellite Altimetry and Earth Sciences: A Handbook of Techniques and Application*, *Int. Geophys. Ser.*, vol. 69, 463 pp., Academic, San Diego, Calif.

Gill, A. E. (1982), *Atmosphere-Ocean Dynamics*, 662 pp., Academic, San Diego, Calif.

Häkkinen, S., and G. L. Mellor (1992), Modeling the seasonal variability of the coupled Arctic ice-ocean system, *J. Geophys. Res.*, *97*, 20,285–20,304, doi:10.1029/92JC02037.

Holland, D. M., R. H. Thomas, B. de Young, M. H. Ribergaard, and B. Lyberth (2008), Acceleration of Jakobshawn Isbrae triggered by warm subsurface ocean waters, *Nat. Geosci.*, *1*, 659–664, doi:10.1038/ngeo316.

Ingleby, B., and M. Huddleston (2007), Quality control of ocean temperature at profiles-huistorical and real-time data, *J. Mar. Syst.*, *65*, 158–175, doi:10.1016/j.jmarsys.2005.11.019.

Intergovernmental Panel on Climate Change (2007), *Climate Change 2007: The Physical Science Basis: Working Group I Contribution to the Fourth Assessment Report of the Intergovernmental Panel on Climate Change*, edited by S. Solomon et al., Cambridge Univ. Press, New York.

Ishii, M., and M. Kimoto (2009), Reevaluation of historical ocean heat content variations with varying XBT and MBT depth bias corrections, *J. Oceanogr.*, *65*, 287–299, doi:10.1007/s10872-009-0027-7.

Kalnay, E. C., et al. (1996), The NCEP/NCAR 40-year reanalysis project, *Bull. Am. Meteorol. Soc.*, *77*, 437–471, doi:10.1175/1520-0477(1996)077<0437:TNYRP>2.0.CO;2.

Karcher, M. J., R. Gerdes, F. Kauker, and C. Koberle (2003), Arctic warming: Evolution and spreading of the 1990s warm event in the Nordic seas and the Arctic Ocean, *J. Geophys. Res.*, *108*(C2), 3034, doi:10.1029/2001JC001265.

Köhl, A., and D. Stammer (2008), Decadal sea level changes in the 50-year GECCO ocean synthesis, *J. Clim.*, *21*(9), 1876–1890, doi:10.1175/2007JCLI2081.1.

Kwok, R., G. F. Cunningham, M. Wensnahan, I. Rigor, H. J. Zwally, and D. Yi (2009), Thinning and volume loss of the Arctic Ocean sea ice cover: 2003–2008, *J. Geophys. Res.*, *114*, C07005, doi:10.1029/2009JC005312.

Lawrence, D. M., A. G. Slater, R. A. Tomas, M. M. Holland, and C. Deser (2008), Accelerated Arctic land warming and permafrost degradation during rapid sea ice loss, *Geophys. Res. Lett.*, *35*, L11506, doi:10.1029/2008GL033985.

Lemke, P., et al. (2007), Observations: Changes in snow, ice and frozen ground, in *Climate Change 2007: The Physical Science Basis: Working Group I Contribution to the Fourth Assessment report of the Intergovernmental Panel on Climate Change*, edited by S. Solomon et al., pp. 337–384, Cambridge Univ. Press, New York.

Levitus, S., J. L. Antonov, and T. P. Boyer (2005), Warming of the world ocean, 1955–2003, *Geophys. Res. Lett.*, *32*, L02604, doi:10.1029/2004GL021592.

Levitus, S., J. L. Antonov, T. P. Boyer, R. A. Locarnini, H. E. Garcia, and A. V. Mishonov (2009), Global ocean heat content 1955–2008 in light of recently revealed instrumentation, *Geophys. Res. Lett.*, *36*, L07608, doi:10.1029/2008GL037155.

Lombard, A., A. Cazenave, P. Y. Le Traon, and M. Ishii (2005), Contribution of thermal expansion to present-day sea-level change revisited, *Global Planet. Change*, *47*(1), 1–16, doi:10.1016/j.gloplacha.2004.11.016.

Milne, G., W. R. Gehrels, C. Hughes, and M. Tamisiea (2009), Identifying the causes of sea level changes, *Nat. Geosci.*, *2*, 471–478, doi:10.1038/ngeo544.

Paulson, A., S. Zhong, and J. Wahr (2007), Inference of mantle viscosity from GRACE and relative sea level data, *Geophys. J. Int.*, *171*, 497–508, doi:10.1111/j.1365-246X.2007.03556.x.

Peltier, W. R. (2004), Global glacial isostasy and the surface of the ice-age Earth: The ICE-5G (VM2) model and GRACE, *Annu. Rev. Earth Planet. Sci.*, *32*, 111–149, doi:10.1146/annurev.earth.32.082503.144359.

Peltier, W. R. (2009), Closure of the budget of global sea level rise over the GRACE era: The importance and magnitudes of the required corrections for global isostatic adjustment, *Quat. Sci. Rev.*, *28*, 1658–1674, doi:10.1016/j.quascirev.2009.04.004.

Peltier, W. R., and S. B. Luthcke (2009), On the origins of Earth rotation anomalies: New insights on the basis of both "paleogeodetic" data and Gravity Recovery and Climate Experiment (GRACE) data, *J. Geophys. Res.*, *114*, B11405, doi:10.1029/2009JB006352.

Polyakov, I. V., et al. (2005), One more step toward a warmer Arctic, *Geophys. Res. Lett.*, *32*, L17605, doi:10.1029/2005GL023740.

Ponte, R. M. (2006), Low-frequency sea level variability and the inverted barometer effect, *J. Atmos. Oceanic Technol.*, *23*(4), 619–629, doi:10.1175/JTECH1864.1.

Prandi, P., M. Ablain, A. Cazenave, and N. Picot (2012), A new estimation of mean sea level in the Arctic Ocean from satellite altimetry, *Mar. Geod.*, in press.

Preisendorfer, R. W. (1988), *Principal Component Analysis in Meteorology and Oceanography*, *Dev. Atmos. Sci. Ser.*, Vol. 17, Elsevier, Amsterdam.

Proshutinsky, A., V. Pavlov, and R. H. Bourke (2001), Sea level rise in the Arctic Ocean, *Geophys. Res. Lett.*, *28*(11), 2237–2240, doi:10.1029/2000GL012760.

Proshutinsky, A., I. M. Ashik, E. N. Dvorkin, S. Häkkinen, R. A. Krishfield, and W. R. Peltier (2004), Secular sea level change in the Russian sector of the Arctic Ocean, *J. Geophys. Res.*, *109*, C03042, doi:10.1029/2003JC002007.

Proshutinsky, A., I. Ashik, S. Häkkinen, E. Hunke, R. Krishfield, M. Maltrud, W. Maslowski, and J. Zhang (2007a), Sea level variability in the Arctic Ocean from AOMIP models, *J. Geophys. Res.*, *112*, C04S08, doi:10.1029/2006JC003916.

Proshutinsky, A., et al. (2007b), The Arctic Ocean, *Bull. Am. Meteorol. Soc.*, *89*, supplement, S86–S89.

Proshutinsky, A., et al. (2009), Ocean, *Bull. Am. Meteorol. Soc.*, *90*, supplement, S99–S102.

Proshutinsky, A., et al. (2011), The Arctic (Ocean), *Bull. Am. Meteorol. Soc.*, *92*(6), supplement, S145–S148.

Rignot, E., I. Velicogna, M. R. van den Broeke, A. Monaghan, and J. Lenaerts (2011), Acceleration of the contribution of the Greenland and Antarctic ice sheets to sea level rise, *Geophys. Res. Lett.*, *38*, L05503, doi:10.1029/2011GL046583.

Rigor, I. G., and J. M. Wallace (2004), Variations in the age of Arctic sea-ice and summer sea-ice extent, *Geophys. Res. Lett.*, *31*, L09401, doi:10.1029/2004GL019492.

Roy, K., and W. R. Peltier (2011), GRACE era secular trends in Earth rotation parameters: A global scale impact of the global warming process?, *Geophys. Res. Lett.*, *38*, L10306, doi:10.1029/2011GL047282.

Serreze, M. C., and R. G. Barry (2011), Processes and impacts of Arctic amplification: A research synthesis, *Global Planet. Change*, *77*(1–2), 85–96, doi:10.1016/j.gloplacha.2011.03.004.

Smith, L. C., Y. Sheng, G. M. MacDonald, and L. D. Hinzman (2005), Disappearing arctic lakes, *Science*, *308*, 1429, doi:10.1126/science.1108142.

Steffen, K. et al. (2010), Cryospheric contributions to sea level rise and variability, in *Understanding Sea-Level Rise and Variability*, edited by J. Church et al., pp. 177–225, Blackwell, Oxford, U. K., doi:10.1002/9781444323276.ch7.

Stroeve, J., M. M. Holland, W. Meier, T. Scambos, and M. Serreze (2007), Arctic sea ice decline: Faster than forecast, *Geophys. Res. Lett.*, *34*, L09501, doi:10.1029/2007GL029703.

Tamisiea, M. E., and J. X. Mitrovica (2011), The moving boundaries of sea level change: Understanding the origins of geographic variability, *Oceanography*, *24*(2), 24–39, doi:10.5670/oceanog.2011.25.

Vestøl, O. (2006), Determination of postglacial land uplift in Fennoscandia from leveling, tide gauges and continuous GPS stations using least-squares collocation, *J. Geod.*, *80*, 248–258, doi:10.1007/s00190-006-0063-7.

Wahr, J., S. Swenson, V. Zlotnicki, and I. Velicogna (2004), Time-variable gravity from GRACE: First results, *Geophys. Res. Lett.*, *31*, L11501, doi:10.1029/2004GL019779.

Wijffels, S. E., J. Willis, C. M. Domingues, P. Barker, N. J. White, A. Gronell, K. Ridgway, and J. A. Church (2008), Changing expendable bathythermograph fall rates and their impact on estimates of thermosteric sea level rise, *J. Clim.*, *21*, 5657–5672, doi:10.1175/2008JCLI2290.1.

Woodworth, P. L., and R. Player (2003), The permanent service for mean sea level: An update to the 21st century, *J. Coastal Res.*, *19*, 287–295.

Wunsch, C., and D. Stammer (1997), Atmospheric loading and the oceanic "inverted barometer" effect, *Rev. Geophys.*, *35*(1), 79–107, doi:10.1029/96RG03037.

Wunsch, C., R. M. Ponte, and P. Heimbach (2007), Decadal trends in sea level patterns: 1993–2004, *J. Clim.*, *20*(24), 5889–5911, doi:10.1175/2007JCLI1840.1.